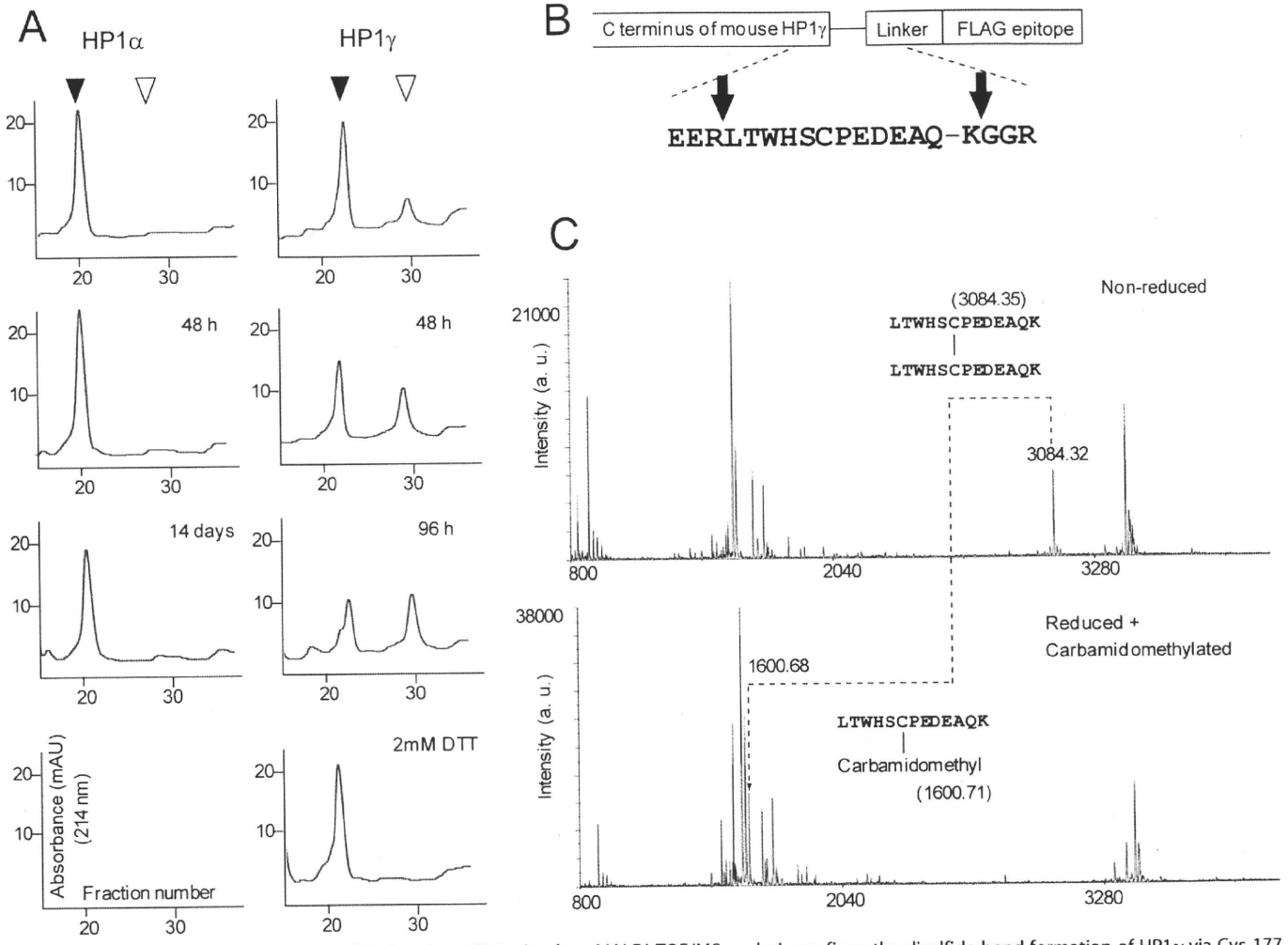


FIGURE 3. **HP1γ is more sensitive to oxidation than HP1α *in vitro*.** MALDI-TOF/MS analysis confirms the disulfide bond formation of HP1γ via Cys-177. *A*, HP1α-FLAG or HP1γ-FLAG expressed in COS7 cells was purified by an anion-exchange column and further fractionated by reverse-phase HPLC. The HPLC absorption pattern profiles at 214 nm are shown. *Black* or *white arrowheads* indicate the fraction of hydrophilic (monomer) or hydrophobic (dimer) forms of HP1, respectively. HP1α-FLAG was fractionated by reverse-phase HPLC immediately after anion exchange (*left top*) or after air oxidation at 4 °C for 48 h or 14 days. HP1γ-FLAG was fractionated immediately after anion exchange (*right top*) or after air oxidation at 4 °C for 48 or 96 h. The HP1γ-FLAG oxidized for 6 days was incubated with 2 mM DTT at 4 °C for 1 h and fractionated by reverse-phase HPLC (*right bottom*). *B*, C-terminal structure of HP1γ-FLAG. *Arrowheads* indicate the trypsin digestion positions. *C*, mass spectra from MALDI-TOF/MS analysis of nonreduced (*upper panel*) or reduced, carbamidomethylated (*lower panel*) HP1γ-FLAG. The expected sequence and estimated mass (*m/z*) of the digested peptide are shown.

was rapidly formed within minutes and was only formed via Cys-177 (Fig. 4*C*). The I165E mutation, which inhibits both noncovalent α-helix dimer formation and proper nuclear localization (6–7), decreased, but not completely, the amount of disulfide dimers of HP1γ (supplemental Fig. S3*A*). These data suggest that the oxidative dimerization of HP1γ requires the proper localization and formation of constitutive, noncovalent dimers.

In contrast to HP1γ, an increase in dimerized HP1α was not observed under the same *in vivo* oxidative conditions (Fig. 4*B*, *right panel*). The dimerized forms of HP1α and HP1γ under basal conditions were almost undetectable without using the large scale purification shown in Fig. 1 because of their relatively low abundance before oxidant treatment. Menadione treatment promoted HP1γ dimerization in various cells, but the extent of dimerization varied among cell types (supplemental Fig. S3*B*), suggesting that the reactivity of HP1γ to reactive oxygen species stimulation varied according to cell type. In each cell, an increase in dimerized HP1α was not observed (data not shown). These results demonstrate that there is a clear difference in oxidation sensitivity among HP1 family members. Although both HP1α and HP1γ have oxidation-sensitive cysteines in their sequences, HP1γ perceives oxidative conditions and is able to more readily form a disulfide dimer than HP1α.

In HEK293T cells, the dimerized HP1γ was subsequently reduced to the monomer form after removal of the oxidant (Fig. 4*D*, *upper panel*), but HP1γ remained dimerized when continuously exposed to the oxidants (Fig. 4*D*, *lower panel*), suggesting that this oxidative modification was reversible.

$H_2O_2$, known as an endogenous source of reactive oxygen species, also promoted dimerization of HP1γ (Fig. 4*E*). This effect of $H_2O_2$ was relatively weak in HEK293T cells when compared with the treatment of menadione. However, the same concentration of $H_2O_2$ substantially increased the amount of dimerized HP1γ in HUVECs (Fig. 4*E*, *lower panel*). Therefore, we further examined the molecular characteristics of the disulfide dimerization of HP1γ using HUVECs.

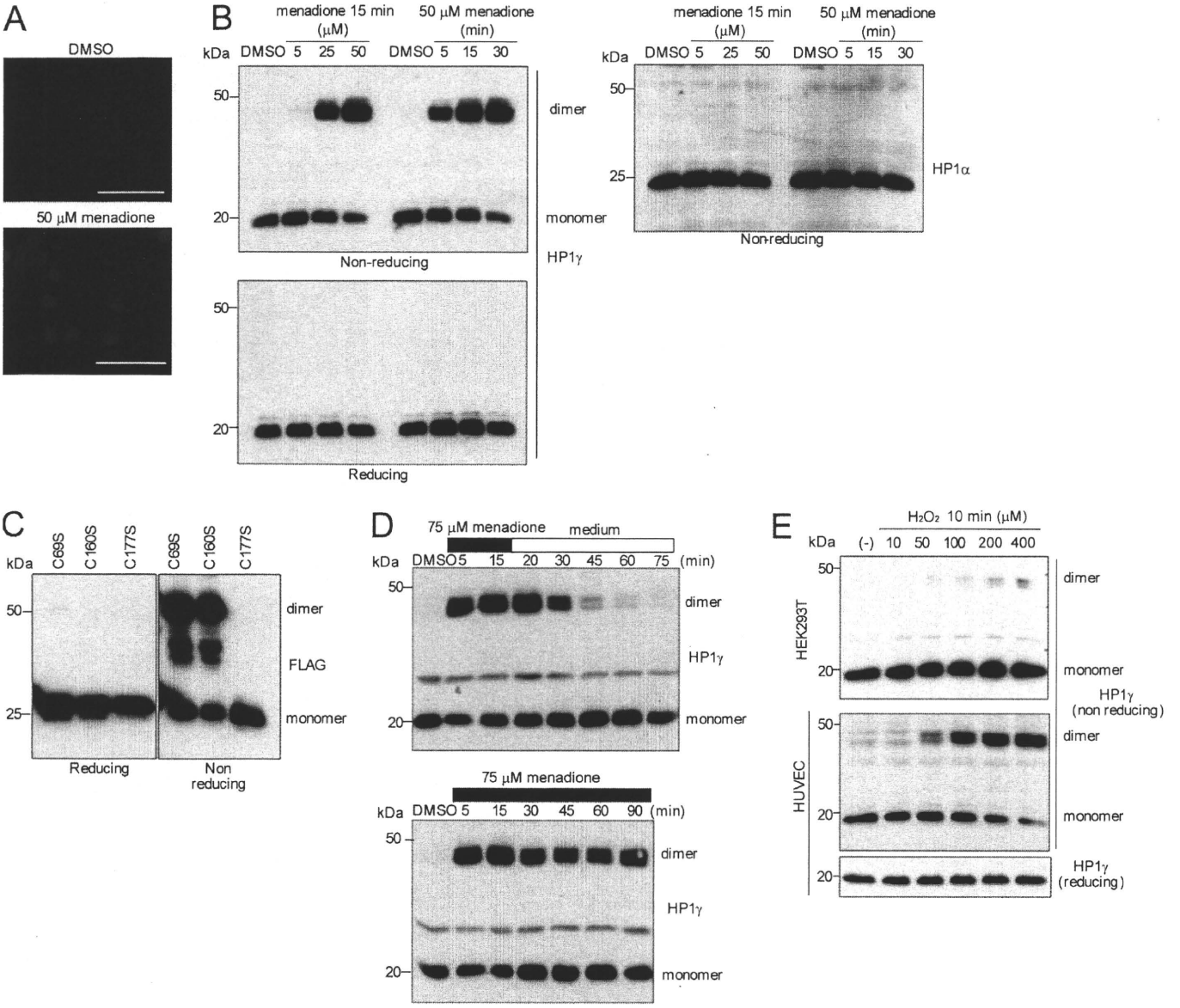


FIGURE 4. **HP1γ, but not HP1α, readily forms disulfide bonds under oxidative conditions.** *A*, after treatment with DMSO or 50 μM menadione for 15 min, COS7 cells were stained with 20 μM dihydroethidium for 30 min and monitored by fluorescence microscopy. *Bar*, 100 μm. *B*, COS7 cells treated with DMSO or menadione under the indicated conditions were lysed, resolved by nonreducing (*upper panel*) or reducing (*lower panel*) SDS-PAGE, and probed with anti-HP1γ antibody. The same membrane was reprobed with anti-HP1α antibody (*right panel*). *C*, COS7 cells expressing each cysteine-to-serine mutant HP1γ-FLAG were treated with 50 μM menadione for 15 min. Lysates were resolved by reducing (*left panel*) or nonreducing (*right panel*) SDS-PAGE and probed with anti-FLAG antibody. *D*, HEK293T cells were treated with 75 μM menadione for 15 min. Subsequently, the culture medium was exchanged for fresh medium (*upper panel*) or kept unchanged (*lower panel*). After incubation for the indicated time, cell lysates were resolved by nonreducing SDS-PAGE and probed with anti-HP1γ antibody. *E*, HEK293T cells and HUVECs were treated with $H_2O_2$ under the indicated conditions. Cell lysates were resolved by SDS-PAGE and probed with anti-HP1γ antibody. *B–E*, cells were lysed with a buffer (10 mM Tris-HCl, pH 7.2, 150 mM NaCl, 1 mM EDTA, and 1% Nonidet P-40) containing 100 mM maleimide, a thiol-alkylating agent, to prevent artifactual oxidation.

*Under Oxidative Conditions, HP1γ Strongly and Transiently Interacts with TIF1β and Holds It in a Chromatin Component*—The CSD of HP1, which includes Cys-177 at its C terminus, creates a binding surface for other proteins (27). Therefore, disulfide modification of HP1γ may affect the interactions between HP1 and HP1-binding proteins. Because many candidate effectors that bind to HP1 exist (8), we screened the interacting proteins of HP1γ under oxidative conditions using metabolically radiolabeled HUVECs expressing recombinant HP1γ-FLAG transduced with adenovirus. Among the co-immunoprecipitated proteins, one protein band was detected after treatment with $H_2O_2$ (Fig. 5*A*, *arrowhead*). The bound protein was purified and analyzed by MALDI-TOF/MS. The amino acid sequence of the digested peptides corresponded to TIF1β (also known as TRIM28 or KAP1), which is a universal co-repressor of gene transcription and is a well known interacting partner of HP1 (28–31). Co-immunoprecipitation analysis showed that endogenous HP1γ strongly interacted with TIF1β in a dose-dependent manner after $H_2O_2$ treatment (Fig. 5*B*). TIF1β did not interact with HP1γ with a C177S mutation under oxidative conditions, suggesting that the disulfide bond formation of HP1γ enhanced the interaction of these proteins (Fig. 5*C*). When the oxidant was removed, TIF1β dissociated again from HP1γ, suggesting that this enhanced endogenous interac-

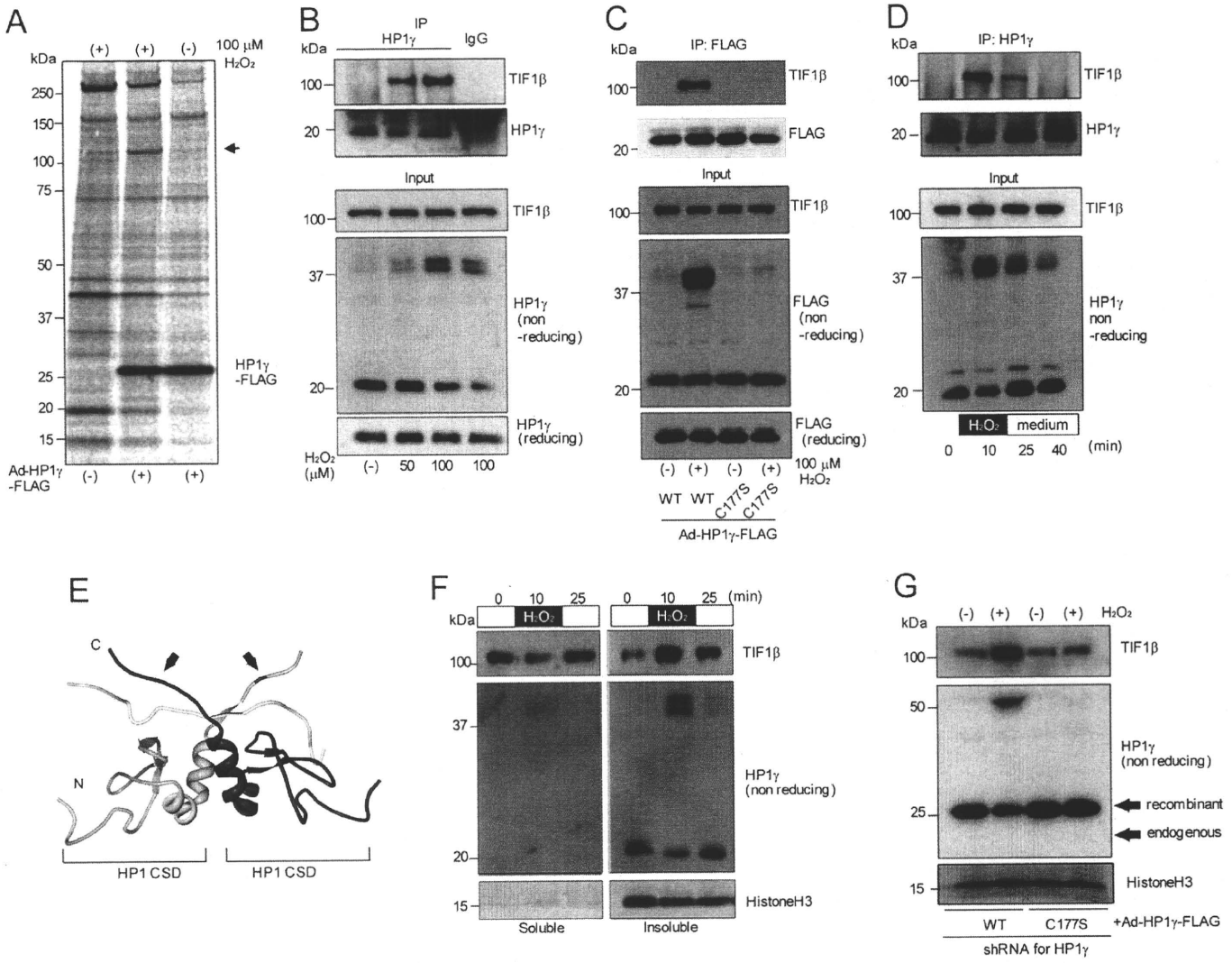


FIGURE 5. **HP1γ strongly interacts with TIF1β and promotes translocation of TIF1β to a chromatin component when dimerized under oxidative conditions.** *A*, HUVECs expressing HP1γ-FLAG (transduced by adenovirus) were metabolically labeled with [$^{35}$S]cysteine and -methionine for 6 h. Nontransduced cells were also labeled as a negative control. Forty eight h after transduction, the cells were treated with 100 μM $H_2O_2$ or control (water) for 10 min, lysed, and immunoprecipitated with anti-FLAG M2 affinity gel. Bound samples were resolved by reducing SDS-PAGE and visualized by autoradiography. The *arrow* indicates the protein band co-immunoprecipitated with HP1γ-FLAG only under the oxidative conditions. *B*, lysates from HUVECs treated with control (water) or $H_2O_2$ for 10 min were immunoprecipitated (*IP*) with anti-HP1γ antibody. Bound samples were resolved by SDS-PAGE and probed with the indicated antibodies. *C*, HUVECs expressing WT or C177S HP1γ-FLAG (transduced by adenovirus) were treated with 100 μM $H_2O_2$ for 10 min. Lysates were immunoprecipitated with anti-FLAG M2 affinity gel, and bound samples were resolved by SDS-PAGE and probed with the indicated antibodies. *D*, HUVECs were transiently treated with 100 μM $H_2O_2$. Lysates were immunoprecipitated with anti-HP1γ antibody, and bound samples were resolved by SDS-PAGE and probed with the indicated antibodies. *E*, structure of HP1 CSD noncovalent homodimer (*blue* and *cyan*) and PXVXL motif (*yellow*) complex (Protein Data Bank code 1s4z, modified using the WEB tool (43)). The position of Cys-177 in HP1γ is highlighted in *red* (*black arrows*). *F*, HUVECs were transiently treated with 100 μM $H_2O_2$. Soluble and insoluble nuclear fractions were obtained using Triton extraction. Each sample was resolved by SDS-PAGE and probed with the indicated antibodies. *G*, HUVECs were transduced with lentivirus expressing shRNA against HP1γ and adenovirus expressing shRNA-resistant HP1γ-FLAG WT or C177S mutant. Triton-insoluble fractions from these cells after $H_2O_2$ treatment were resolved by SDS-PAGE and probed with the indicated antibodies.

tion was transient (Fig. 5*D*). Structurally, disulfide dimerization via Cys-177 is formed at the C terminus of the CSD, just adjacent to the binding interface for the PXVXL motif, which is a well characterized binding sequence in HP1-interacting proteins, including TIF1β (Fig. 5*E*) (7).

We next examined the localization changes of these proteins before and after oxidant treatment. No remarkable change in localization was detected by immunostaining (data not shown). However, biochemical analysis using Triton extraction verified the TIF1β translocation. HP1γ existed mainly in the Triton-insoluble chromatin component, whereas TIF1β was distributed both in the soluble and the insoluble components (Fig. 5*F*). Under oxidative conditions, HP1γ dimerized and was maintained in the insoluble components. Concomitant with HP1γ dimerization, the insoluble component of TIF1β transiently increased. The knockdown of endogenous HP1γ combined with the replacement by a C177S mutant of HP1γ inhibited the translocation of TIF1β, suggesting that HP1γ held TIF1β on chromatin only when oxidized via Cys-177 (Fig. 5*G*). These data suggest that the intracellular redox state is transduced to the conformational and localization change of the repressor complex via oxidative modification of HP1γ.

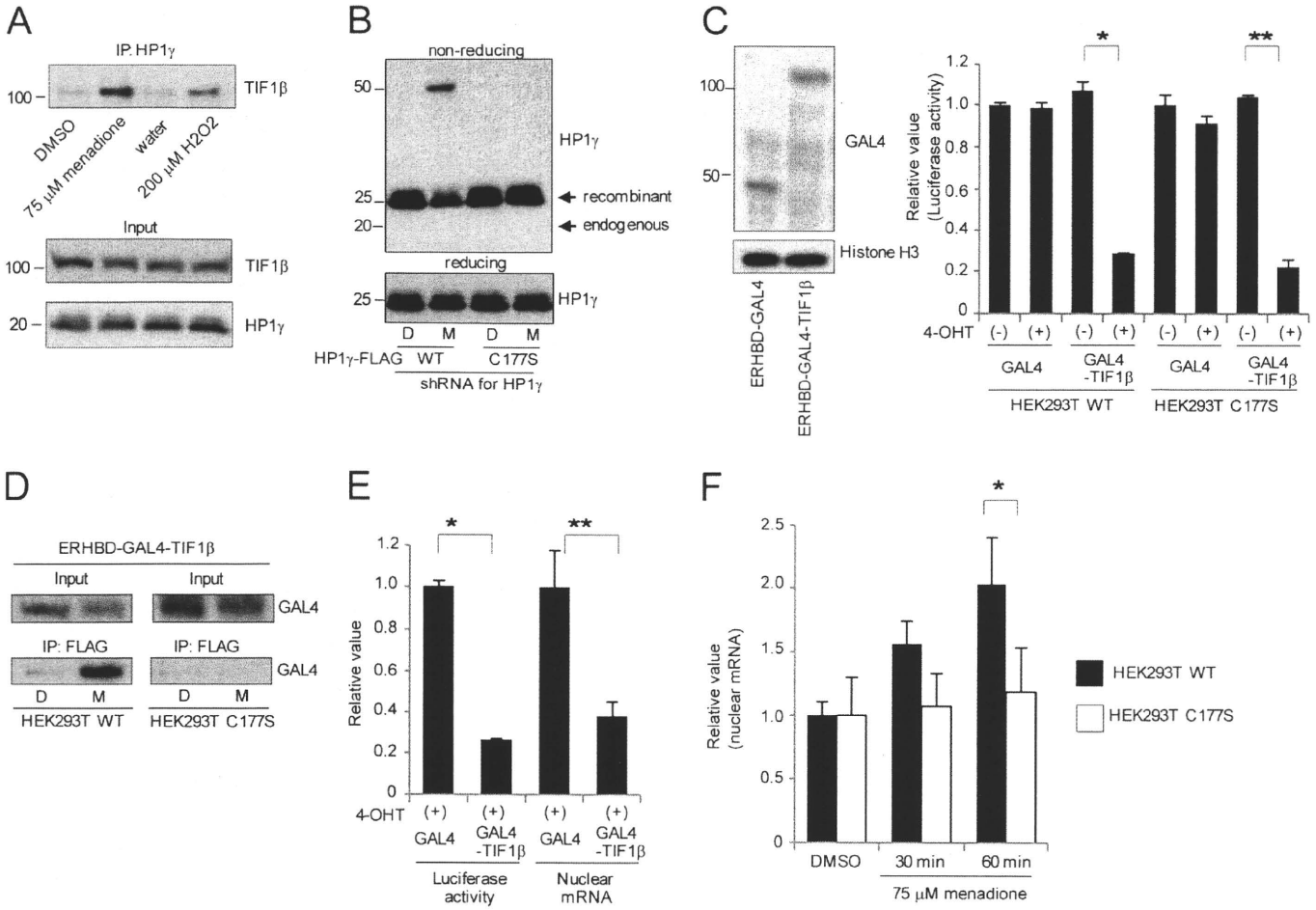


FIGURE 6. **Dimerized HP1γ under oxidative conditions inhibits the repression ability of TIF1β.** *A*, lysates from HEK293T cells treated with DMSO, 75 μM menadione, water, or 200 μM $H_2O_2$ for 15 min were immunoprecipitated (*IP*) with anti-HP1γ antibody. Bound samples were resolved by SDS-PAGE and probed with the indicated antibodies. *B*, HEK293T cells stably expressing shRNA for HP1γ and shRNA-resistant recombinant FLAG-tagged HP1γ were treated with DMSO or 75 μM menadione for 15 min. Cell lysates were resolved by nonreducing or reducing SDS-PAGE and probed with anti-HP1γ antibody. *D* indicates DMSO, and *M* indicates 75 μM menadione. *C*, lysates from HEK293T stable cells transfected with an ERHBD-GAL4 or ERHBD-GAL4-TIF1β fusion protein were resolved by SDS-PAGE and probed with the indicated antibodies (*left panel*). HEK293T stable cells were transfected with the plasmids encoding ERHBD-GAL4 or ERHBD-GAL4-TIF1β with the reporter plasmids. Twenty four h after transfection, 4-OHT was added to culture medium (500 nM). Forty eight h after transfection, luciferase activity was measured (*right panel*). The relative value was corrected by the value of the cells transfected with ERHBD-GAL4 without 4-OHT induction. Student's *t* test; *, **, $p < 0.01$. *D*, HEK293T stable cells expressing ERHBD-GAL4-TIF1β were treated with DMSO or 75 μM menadione for 15 min. Lysates were immunoprecipitated with anti-FLAG affinity gel. Bound samples were immunoblotted with anti-GAL4 antibody. *D* indicates DMSO, and *M* indicates 75 μM menadione. *E*, under the same conditions as *C*, luciferase transcription levels were determined both by protein enzymatic activity and intranuclear mRNA levels measured by quantitative PCR. Student's *t* test; *, **, $p < 0.01$. *F*, HEK293T stable cells expressing ERHBD-GAL4-TIF1β with 500 nM 4-OHT induction were treated with DMSO for 60 min or 75 μM menadione for the indicated time. Intranuclear luciferase mRNA levels at each time point were measured by quantitative PCR. The relative value was corrected by the value of the cells treated with DMSO. Two-way repeated measure analysis of variance; *, $p < 0.05$. The means ± S.D. as indicated by the *error bars* were determined from three independent experiments.

*Dimerized HP1γ under Oxidative Conditions Inhibits the Repression Ability of TIF1β*—To clarify whether the repression ability of TIF1β was promoted or inhibited when trapped by HP1γ under oxidative conditions, we used a GAL4-based transcriptional reporter assay. In HEK293T cells, menadione treatment promoted the disulfide dimerization of HP1γ and the interaction between HP1γ and TIF1β more prominently than $H_2O_2$ treatment (supplemental Fig. S3*B* and Figs. 4*E* and 6*A*). Therefore, we used menadione treatment for further analysis in HEK293T cells. We generated HEK293T cells stably expressing shRNA for HP1γ and shRNA-resistant recombinant FLAG-tagged HP1γ WT or C177S mutant. In these cells, endogenous HP1γ was almost completely depleted and was replaced by the dimerizable or undimerizable recombinant proteins (Fig. 6*B*). To evaluate the transcriptional repression ability of TIF1β, we transfected the plasmids encoding ERHBD-GAL4 as a control or ERHBD-GAL4-TIF1β fusion protein with the reporter plasmids in these cells (12, 32). The transcriptional regulatory activity of the ERHBD fusion protein is post-translationally controlled by the addition of 4-OHT to the culture medium (12). In our experimental conditions where ERHBD-GAL4 and ERHBD-GAL4-TIF1β were equally expressed (Fig. 6*C*, *left panel*), only ERHBD-GAL4-TIF1β repressed transcription of luciferase with 4-OHT (500 nM) in the HEK293T stable cells (Fig. 6*C*, *right panel*). The extent of repression was similar between the cells expressing either the HP1γ-FLAG WT or the C177S mutant under nonoxidative conditions. When the cells were treated with menadione, HP1γ-FLAG WT strongly interacted with ERHBD-GAL4-TIF1β as was similarly observed with endogenous proteins (Fig. 6*D*). To examine the transcrip-

tional change of the luciferase gene under oxidative conditions, we measured the intranuclear mRNA levels of luciferase by quantitative PCR instead of luciferase protein enzymatic activity (Fig. 6*E*). We chose this end point because the oxidation of HP1γ was too rapid to properly evaluate its effect on luciferase transcription by measuring luciferase protein enzymatic activity. Under these conditions, menadione treatment relieved the levels of luciferase transcription repressed by ERHBD-GAL4-TIF1β in the cells expressing HP1γ-FLAG WT but did not relieve the levels in the cells expressing the C177S mutant (Fig. 6*F*). These data suggest that dimerized HP1γ under oxidative conditions inhibits the repression ability of TIF1β.

It remained unclear whether the intranuclear redox-sensing mechanism through the oxidative modification of HP1γ plays a role in the cellular response to extrinsic oxidative stress. Therefore, we assessed the effect of this modification on cell survival under oxidative conditions using HEK293T cells stably expressing shRNA against HP1γ (supplemental Fig. S4*A*). Depletion of HP1γ using shRNA uniformly decreased cell viability under oxidative conditions induced by menadione treatment (supplemental Fig. S4*B*). For a rescue experiment, these stable clones were transduced with an adenoviral vector encoding WT HP1γ-FLAG or C177S HP1γ-FLAG. Both HP1γ vectors were cloned from murine cDNA and were resistant to shRNA against human HP1γ. Transduction of both adenoviral constructs at a multiplicity of infection of 20 resulted in nearly equal expression of recombinant HP1γ with endogenous HP1γ and yielded a similar disulfide dimerization pattern (supplemental Fig. S4*C*). Under these conditions, WT HP1γ-FLAG rescued cell viability after menadione treatment in each stable clone, but the C177S HP1γ-FLAG mutant did not rescue cell viability (supplemental Fig. S4*D*). These results suggest that HP1γ disulfide dimerization plays a pivotal role in cell survival under oxidative conditions.

## DISCUSSION

In this study, we identified isoform-specific disulfide bond formation, which is a novel post-translational modification of HP1, using a unique column chromatography method. Biochemical analysis revealed two isoform-specific reactive cysteine residues, cysteine 133 in HP1α and cysteine 177 in HP1γ. In particular, HP1γ readily and reversibly formed disulfide dimers under oxidative conditions. Dimerized HP1γ strongly interacted with TIF1β and held it in a chromatin component. The GAL4 tethering repression assay revealed that the tight interaction of the repressor proteins had a reversing effect for transcriptional repression.

Several post-translational modifications of HP1 have been reported. Specifically, the linker region between the CSD and CD is highly amenable to post-translational modifications, especially phosphorylation that affects silencing activity or nuclear location of HP1 (17, 33–35). Also in the CD, Thr-51 of HP1β has been shown to be phosphorylated in response to DNA damage (22). More recently, a comprehensive proteomic analysis revealed that all HP1 isoforms are highly modified by phosphorylation, acetylation, methylation, and formylation both in the CD and in the CSD (36). Prior to this study, however, no oxidative modification of HP1 had been identified. Because oxidative modifications at cysteine residues would be easily disrupted under reducing conditions, such modifications may be detected only by the unique HPLC-based method used in this study and not by ordinary mass spectrometry analysis.

Both isoform-specific cysteines involved in forming disulfide bonds reside in a structurally flexible region of the CSD. Cys-133 of HP1α lies in the long loop between the β1 and β2 sheets, and Cys-177 of HP1γ lies in the C-terminal region. Introducing cysteine residues into these flexible sites of HP1β conferred the ability to form disulfide bonds, suggesting that these sites have specific structures in the oxidative center. Although both cysteines were reactive, a distinct difference of sensitivity to oxidation existed. Each location of reactive cysteines and the surrounding structure might determine the sensitivity of HP1α and -γ to oxidation. Under both *in vitro* and *in vivo* oxidative conditions, HP1γ readily formed disulfide bonds. In contrast, only minimal disulfide formation of HP1α by oxidation was observed under our experimental conditions. The reactivity of HP1α under oxidation might be observed under different conditions. Nonetheless, the isoform specificity and functional importance of Cys-133 in HP1α has been reported previously (15).

HP1 has been reported to form dimers via the CSD, but these dimers are not mediated by disulfide bonds or other covalent bonds (6, 37, 38). Thus, HP1 dimerizes in at least two ways. The interface of the noncovalently linked dimer involves a symmetrical interaction on helix α2 of the CSD (27) and creates a nonpolar groove structure, which is a binding site for the P*X*VXL motif in HP1-interacting proteins, such as TIF1β (Fig. 5*E*) (7). Because reactive cysteine 177 in HP1γ is located in the C terminus adjacent to the groove structure, disulfide bond formation at this site likely affects the binding affinity of HP1γ. Indeed, HP1γ strongly and transiently interacted with TIF1β and promoted its translocation to a chromatin component stringently depending on the oxidative status of cysteine 177. This rapid reacting mechanism to transduce cellular redox state to a conformational change like a clear "on-off switch" suggests that HP1γ is a functional redox sensor.

During the cellular response to oxidative stress, an increase in oxidants can trigger alterations in transcription levels through direct activation or by promoting a change in the subcellular localization of transcription factors by oxidizing reactive cysteine residues (25). Among these oxidative responses, the disulfide dimerization of HP1γ demonstrated in this study appears to be one of the most rapid transcriptional regulatory mechanisms. TIF1β is a universal co-repressor for the Krüppel-associated box domain containing the zinc finger protein (KRAB-ZNF) family of transcription factors, and it is the major protein binding the CSD of HP1 (28–31). TIF1β also works as a scaffold for the repressor complex, and its interaction with HP1 is essential for its repression activity (12, 39–41). Recent findings have revealed that the binding of HP1 to TIF1β is essential for their coordinated function on the promoter of the endogenous genes (42). Therefore, the reversing effect for the repressive ability of TIF1β caused by HP1γ disulfide dimerization might be required for a short period of adaptation against oxidative stress. Downstream genes regulated by these scaffold complexes remain to be clarified in the future analysis.

In conclusion, our study suggests that HP1 potentially acts as a rapid redox sensor, and it may connect the intracellular redox state with transcriptional regulation under various physiological conditions.

*Acknowledgments—We thank David C. Schultz and Takahiro Nagase for the plasmid constructs. We thank Saori Ikezawa and Yoko Hamada for technical assistance and Yasunori Shintani for thoughtful discussions.*

## REFERENCES


1. James, T. C., and Elgin, S. C. (1986) *Mol. Cell. Biol.* **6,** 3862–3872
2. Wallrath, L. L. (1998) *Curr. Opin. Genet. Dev.* **8,** 147–153
3. Bannister, A. J., Zegerman, P., Partridge, J. F., Miska, E. A., Thomas, J. O., Allshire, R. C., and Kouzarides, T. (2001) *Nature* **410,** 120–124
4. Nakayama, J., Rice, J. C., Strahl, B. D., Allis, C. D., and Grewal, S. I. (2001) *Science* **292,** 110–113
5. Lachner, M., O'Carroll, D., Rea, S., Mechtler, K., and Jenuwein, T. (2001) *Nature* **410,** 116–120
6. Brasher, S. V., Smith, B. O., Fogh, R. H., Nietlispach, D., Thiru, A., Nielsen, P. R., Broadhurst, R. W., Ball, L. J., Murzina, N. V., and Laue, E. D. (2000) *EMBO J.* **19,** 1587–1597
7. Thiru, A., Nietlispach, D., Mott, H. R., Okuwaki, M., Lyon, D., Nielsen, P. R., Hirshberg, M., Verreault, A., Murzina, N. V., and Laue, E. D. (2004) *EMBO J.* **23,** 489–499
8. Grewal, S. I., and Jia, S. (2007) *Nat. Rev. Genet.* **8,** 35–46
9. Lomberk, G., Wallrath, L., and Urrutia, R. (2006) *Genome Biol.* **7,** 228
10. Schultz, D. C., Ayyanathan, K., Negorev, D., Maul, G. G., and Rauscher, F. J., 3rd. (2002) *Genes Dev.* **16,** 919–932
11. Maison, C., and Almouzni, G. (2004) *Nat. Rev. Mol. Cell Biol.* **5,** 296–304
12. Sripathy, S. P., Stevens, J., and Schultz, D. C. (2006) *Mol. Cell. Biol.* **26,** 8623–8638
13. Cammas, F., Janoshazi, A., Lerouge, T., and Losson, R. (2007) *Differentiation* **75,** 627–637
14. Filesi, I., Cardinale, A., van der Sar, S., Cowell, I. G., Singh, P. B., and Biocca, S. (2002) *J. Cell Sci.* **115,** 1803–1813
15. Nielsen, A. L., Sanchez, C., Ichinose, H., Cerviño, M., Lerouge, T., Chambon, P., and Losson, R. (2002) *EMBO J.* **21,** 5797–5806
16. Vassallo, M. F., and Tanese, N. (2002) *Proc. Natl. Acad. Sci. U.S.A.* **99,** 5919–5924
17. Lomberk, G., Bensi, D., Fernandez-Zapico, M. E., and Urrutia, R. (2006) *Nat. Cell Biol.* **8,** 407–415
18. Gilbert, N., Boyle, S., Sutherland, H., de Las Heras, J., Allan, J., Jenuwein, T., and Bickmore, W. A. (2003) *EMBO J.* **22,** 5540–5550
19. Ritou, E., Bai, M., and Georgatos, S. D. (2007) *J. Cell Sci.* **120,** 3425–3435
20. Mateescu, B., Bourachot, B., Rachez, C., Ogryzko, V., and Muchardt, C. (2008) *EMBO Rep.* **9,** 267–272
21. Vakoc, C. R., Mandat, S. A., Olenchock, B. A., and Blobel, G. A. (2005) *Mol. Cell* **19,** 381–391
22. Ayoub, N., Jeyasekharan, A. D., Bernal, J. A., and Venkitaraman, A. R. (2008) *Nature* **453,** 682–686
23. Petta, T. B., Nakajima, S., Zlatanou, A., Despras, E., Couve-Privat, S., Ishchenko, A., Sarasin, A., Yasui, A., and Kannouche, P. (2008) *EMBO J.* **27,** 2883–2895
24. Asano, Y., Takashima, S., Asakura, M., Shintani, Y., Liao, Y., Minamino, T., Asanuma, H., Sanada, S., Kim, J., Ogai, A., Fukushima, T., Oikawa, Y., Okazaki, Y., Kaneda, Y., Sato, M., Miyazaki, J., Kitamura, S., Tomoike, H., Kitakaze, M., and Hori, M. (2004) *Nat. Genet.* **36,** 123–130
25. D'Autréaux, B., and Toledano, M. B. (2007) *Nat. Rev. Mol. Cell Biol.* **8,** 813–824
26. Oka, S., Ohno, M., Tsuchimoto, D., Sakumi, K., Furuichi, M., and Nakabeppu, Y. (2008) *EMBO J.* **27,** 421–432
27. Cowieson, N. P., Partridge, J. F., Allshire, R. C., and McLaughlin, P. J. (2000) *Curr. Biol.* **10,** 517–525
28. Friedman, J. R., Fredericks, W. J., Jensen, D. E., Speicher, D. W., Huang, X. P., Neilson, E. G., and Rauscher, F. J., 3rd. (1996) *Genes Dev.* **10,** 2067–2078
29. Kim, S. S., Chen, Y. M., O'Leary, E., Witzgall, R., Vidal, M., and Bonventre, J. V. (1996) *Proc. Natl. Acad. Sci. U.S.A.* **93,** 15299–15304
30. Le Douarin, B., Nielsen, A. L., Garnier, J. M., Ichinose, H., Jeanmougin, F., Losson, R., and Chambon, P. (1996) *EMBO J.* **15,** 6701–6715
31. Moosmann, P., Georgiev, O., Le Douarin, B., Bourquin, J. P., and Schaffner, W. (1996) *Nucleic Acids Res.* **24,** 4859–4867
32. Itokawa, Y., Yanagawa, T., Yamakawa, H., Watanabe, N., Koga, H., and Nagase, T. (2009) *Biochem. Biophys. Res. Commun.* **388,** 689–694
33. Koike, N., Maita, H., Taira, T., Ariga, H., and Iguchi-Ariga, S. M. (2000) *FEBS Lett.* **467,** 17–21
34. Zhao, T., Heyduk, T., and Eissenberg, J. C. (2001) *J. Biol. Chem.* **276,** 9512–9518
35. Badugu, R., Yoo, Y., Singh, P. B., and Kellum, R. (2005) *Chromosoma* **113,** 370–384
36. Leroy, G., Weston, J. T., Zee, B. M., Young, N. L., Plazas-Mayorca, M. D., and Garcia, B. A. (2009) *Mol. Cell. Proteomics* **8,** 2432–2442
37. Wang, G., Ma, A., Chow, C. M., Horsley, D., Brown, N. R., Cowell, I. G., and Singh, P. B. (2000) *Mol. Cell. Biol.* **20,** 6970–6983
38. Nielsen, A. L., Oulad-Abdelghani, M., Ortiz, J. A., Remboutsika, E., Chambon, P., and Losson, R. (2001) *Mol. Cell* **7,** 729–739
39. Nielsen, A. L., Ortiz, J. A., You, J., Oulad-Abdelghani, M., Khechumian, R., Gansmuller, A., Chambon, P., and Losson, R. (1999) *EMBO J.* **18,** 6385–6395
40. Ayyanathan, K., Lechner, M. S., Bell, P., Maul, G. G., Schultz, D. C., Yamada, Y., Tanaka, K., Torigoe, K., and Rauscher, F. J., 3rd. (2003) *Genes Dev.* **17,** 1855–1869
41. Smallwood, A., Black, J. C., Tanese, N., Pradhan, S., and Carey, M. (2008) *Nat. Struct. Mol. Biol.* **15,** 318–320
42. Riclet, R., Chendeb, M., Vonesch, J. L., Koczan, D., Thiesen, H. J., Losson, R., and Cammas, F. (2009) *Mol. Biol. Cell* **20,** 296–305
43. Moreland, J. L., Gramada, A., Buzko, O. V., Zhang, Q., and Bourne, P. E. (2005) *BMC Bioinformatics* **6,** 21

Basic Res Cardiol (2010) 105:787–794
DOI 10.1007/s00395-010-0119-y

ORIGINAL CONTRIBUTION

# A histamine $H_2$ receptor blocker ameliorates development of heart failure in dogs independently of $\beta$-adrenergic receptor blockade

**Hiroyuki Takahama · Hiroshi Asanuma · Shoji Sanada · Masashi Fujita · Hideyuki Sasaki · Masakatsu Wakeno · Jiyoong Kim · Masanori Asakura · Seiji Takashima · Tetsuo Minamino · Kazuo Komamura · Masaru Sugimachi · Masafumi Kitakaze**

Received: 21 July 2010 / Revised: 31 August 2010 / Accepted: 2 September 2010 / Published online: 18 September 2010


**Abstract** Histamine has a positive inotropic effect on ventricular myocardium and stimulation of histamine $H_2$ receptors increases the intracellular cAMP level via Gs protein, as dose stimulation of $\beta$-adrenergic receptors, and worsens heart failure. To test whether a histamine $H_2$ receptor blocker had a beneficial effect in addition to $\beta$-adrenergic receptor blockade, we investigated the cardioprotective effect of famotidine, a histamine $H_2$ receptor blocker, in dogs receiving a $\beta$-blocker. We induced heart failure in dogs by rapid ventricular pacing (230 beats/min). Animals received no drugs (control group), famotidine (1 mg/kg daily), carvedilol (0.1 mg/kg daily), or carvedilol plus famotidine. Both cardiac catheterization and echocardiography were performed before and 4 weeks after the initiation of pacing. Immunohistochemical studies showed the appearance of mast cells and histamine in the myocardium after 4 weeks of pacing. In the control group, the left ventricular ejection fraction (LVEF) was decreased after 4 weeks compared with before pacing ($71 \pm 2$ vs. $27 \pm 2\%$, $p < 0.05$) and mean pulmonary capillary wedge pressure (PCWP) was increased ($8 \pm 1$ vs. $19 \pm 3$ mmHg). Famotidine ameliorated the decrease of LVEF and increase of PCWP, while the combination of carvedilol plus famotidine further improved both parameters compared with the carvedilol groups. These beneficial effects of famotidine were associated with a decrease of the myocardial cAMP level. Histamine $H_2$ receptor blockade preserves cardiac systolic function in dogs with pacing-induced heart failure, even in the presence of $\beta$-adrenergic receptor blockade. This finding strengthens the rationale for using histamine $H_2$ blockers in the treatment of heart failure.

**Keywords** Heart failure · Histamine · Histamine $H_2$ receptor blocker · $\beta$-Adrenergic receptor blocker

H. Takahama · M. Wakeno · J. Kim · M. Asakura · M. Kitakaze (✉)
Department of Cardiovascular Medicine, National Cerebral and Cardiovascular Center, Suita, Osaka 565-8565, Japan
e-mail: kitakaze@zf6.so-net.ne.jp

H. Asanuma · H. Sasaki · K. Komamura · M. Sugimachi
Cardiovascular Dynamics Research Institute, National Cerebral and Cardiovascular Center, Suita, Japan

H. Asanuma
Department of Emergency Room Medicine, Kinki University School of Medicine, Osaka-Sayama, Japan

S. Sanada · M. Fujita · S. Takashima · T. Minamino
Department of Cardiovascular Medicine, Osaka University Graduate School of Medicine, Suita, Japan

## Introduction

Chronic heart failure (CHF) is one of the major causes of morbidity and mortality worldwide, and is characterized by neurohormonal imbalances that include activation of the sympathetic nervous system [9, 15]. $\beta$-Adrenergic receptor blockade is a established treatment of CHF because it protects the heart from the harmful effects of the sympathetic nervous system that are partly mediated via cyclic adenosine monophosphate (cAMP)-dependent pathways [2, 34]. Interestingly, histamine $H_2$ receptors are linked to Gs proteins that facilitate the production of cAMP (as are $\beta$-adrenergic receptors) and are expressed in the heart [18, 29, 33]. Histamine has a positive inotropic effect on human ventricular myocardium and chronotropic effects [3, 12], and also autonomic control of the heart [21]. Indeed, we previously reported that famotidine, a histamine $H_2$

receptor blocker, protected the heart against ischemia-reperfusion injury in dogs [1] and also improved both symptoms of CHF and ventricular remodeling in the clinical setting [16]. Although the maximum inotropic effects of substances acting through cAMP were decreased in diseased myocardium [6], famotidine, a histamine $H_2$ receptor blocker, exerts negative effects on cardiac performance [13], the roles of the histamine would have remained unclear in the state of heart failure.

In addition, it is still unclear whether histamine $H_2$ receptor blockers have a protective effect against CHF by reducing the myocardial accumulation of cAMP and whether there is an additive effect of histamine $H_2$ receptor blockade in the presence of $\beta$-adrenergic receptor blockade.

Therefore, we investigated the effect of a histamine $H_2$ receptor blocker on cardiac performance and myocardial cAMP accumulation in dogs with pacing-induced heart failure, and also investigated whether there was an additive effect of combined histamine $H_2$ receptor blocker and $\beta$-blocker therapy on cardiac performance.

## Methods

### Materials

The histamine $H_2$ receptor blocker famotidine was kindly provided by Astellas Pharma Inc. (Tokyo, Japan). Carvedilol, a $\beta$-adrenergic receptor blocker, was obtained from Sigma (St. Louis, MO, USA). Rabbit polyclonal anti-histamine antibody was obtained from Progen (Queensland, Australia).

### Animal preparation

Beagle dogs (Oriental Yeast Co. Ltd., Tokyo, Japan) weighing 8–10 kg were sedated with intravenous sodium pentobarbital at a dose of 25 mg/kg. After intubation with a cuffed endotracheal tube, anesthesia was maintained with 0.5–1% isoflurane and an equal mixture of air and oxygen. Ventilation was provided with a tidal volume of 22 mL/kg at a rate of 15 times per minute. A bipolar pacing lead (Model BT-45P, Star Medical Inc., Tokyo, Japan) was advanced under fluoroscopic guidance through the right jugular vein to the right ventricular (RV) apex and was connected to an external programmable pacemaker (VOO mode; Model SIP-501, Star Medical Inc., Tokyo, Japan) that was implanted in a subcutaneous pocket in the neck. The success of this procedure was confirmed by electrocardiography. Antibiotics were given after surgery, and the dogs were allowed to recover fully. Then heart failure was induced by rapid right ventricular pacing at a rate of 230 beats/min for 4 weeks as the model mimicking heart failure in human, as reported previously [22, 23, 27].

All procedures were performed in conformity with the Guide for the Care and Use of Laboratory Animals (NIH publication No. 85–23, 1996 revision) and were approved by the ethical committee for laboratory animal use of the National Cardiovascular Center in Japan.

### Echocardiography

Transthoracic echocardiography was performed by using an echocardiographic system equipped with a 2–4 MHz phased-array transducer (SONOS 5500, Hewlett Packard, Massachusetts, USA) in conscious dogs before pacemaker implantation and 30 min after the cessation of RV pacing at 4 weeks. Good two-dimensional short-axis views of the left ventricle were obtained at the level of the papillary muscles for guided M-mode measurement of the left ventricular (LV) end-diastolic dimension (LVDd), LV end-systolic dimension (LVDs), LV fractional shortening (LVFS), and LV ejection fraction (LVEF). All measurements were made by two observers, who were blinded to the source of the tracings.

### Hemodynamic studies

LV pressure and mean aortic pressure were measured by pressure amplifiers connected to a pig tail catheter (5F, Terumo Co. Ltd., Tokyo, Japan) that was inserted into the left ventricle from the left femoral artery. Pulmonary capillary wedge pressure (PCWP) was measured with a 7 Fr Swan-Ganz catheter (American Edwards Laboratories, California, USA). LV $dP/dt$ was analyzed using software (Data viewer, Yokogawa Electric Corporation, Tokyo, Japan). These studies were performed both before and after 4 weeks of RV pacing or 4 weeks after pacemaker implantation in the sham group.

### Measurement of the myocardial cAMP level

The myocardial cyclic AMP (cAMP) level was measured as described previously [8]. Briefly, a sample of frozen cardiac muscle was homogenized mechanically in 500 mL of frozen hydrochloric acid (0.1 N) with a mechanical homogenizer. The homogenate was thawed and centrifuged at $5{,}000 \times g$ at room temperature for 15 min and then a 100 mL aliquot of the supernatant was employed to measure cAMP with a sensitive radioimmunoassay (cyclic AMP kit; Yamasa Shoyu Co., Choshi, Japan).

### Immunohistochemical analysis

Immunohistochemical analysis was performed as described previously [24]. Briefly, myocardial tissue samples were fixed in 10% formalin and embedded in paraffin. Then

5-μm-thick sections were cut and preincubated with 3% hydrogen peroxide. Rabbit polyclonal anti-histamine antibody (1:1,000 dilution) was added, and incubation was done at room temperature overnight. Next, the sections were incubated with biotinylated anti-rabbit immunoglobulin for 30 min and subsequently with horseradish peroxidase-labeled streptavidin solution for 30 min. The slides were rinsed in tris-buffered saline after each incubation step. Peroxidase activity was visualized by incubation with diaminobenzidine hydrochloride solution.

### Experimental protocols

*Protocol 1: effects of famotidine on cardiac performance and myocardial cAMP accumulation in dogs with pacing-induced heart failure*

After pacemaker implantation, the dogs were randomly assigned to a sham group ($n = 6$) without pacing, a control group ($n = 7$) with pacing only, and a famotidine group ($n = 5$) with pacing plus the daily oral administration of famotidine (1 mg/kg per day). The dose of famotidine was chosen on the basis of previous reports [30, 36]. Echocardiography and measurement of hemodynamic parameters were performed before and 4 weeks after pacemaker implantation. After the measurement of hemodynamic parameters, myocardial tissue samples were obtained and quickly placed into liquid nitrogen for storage at −80°C until measurement of cAMP levels.

*Protocol 2: effects of famotidine on cardiac performance in dogs with pacing-induced heart failure under β-adrenergic receptor blockade*

Next, we examined the additive effect of histamine $H_2$ receptor blockade on the development of CHF. After pacemaker implantation, the dogs were randomly assigned to a carvedilol group ($n = 6$) that received daily oral administration of carvedilol (0.1 mg/kg per day) or a carvedilol + famotidine group ($n = 6$) that received daily oral administration of both carvedilol (0.1 mg/kg per day) and famotidine (1 mg/kg per day).

### Statistical analysis

Results are expressed as the mean ± SEM. Comparison of time-course changes between the groups was performed by two-way repeated measures analysis of variance (ANOVA). For comparison of mast cell counts and cAMP levels between the groups, the Mann–Whitney $U$ test was performed. A $p$ value $< 0.05$ was considered to represent statistical significance.

## Results

### Mast cells and histamine expression

Mast cells were detected in the myocardium by toluidine blue staining. Consistent with previous reports [8, 26], we observed an increase of mast cells in the failing hearts compared with the number of cells in the sham group (Fig. 1a). Immunohistochemical analysis showed an increase of histamine expression indicating increased degranulation of mast cells in failing hearts compared with the level in the sham group (Fig. 1b).

### Effect of famotidine on cardiac performance and myocardial cAMP in dogs with pacing-induced heart failure

Both mean aortic pressure and heart rate before pacing were similar in the control group (104 ± 5 mmHg and

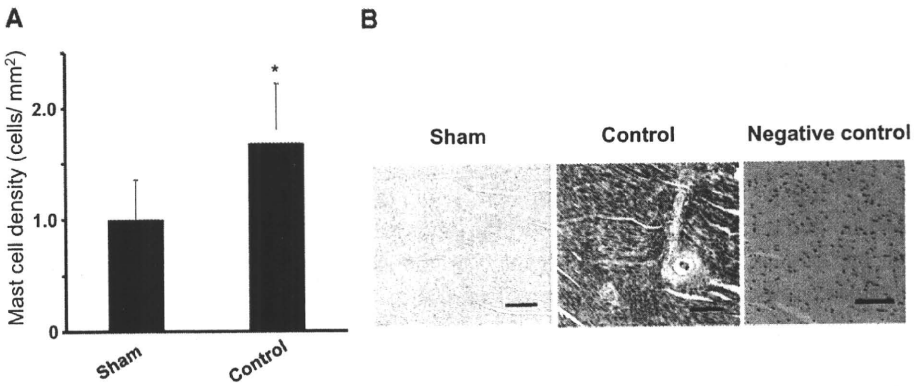


**Fig. 1** Mast cell density and histamine expression in the failing heart. **a** Mast cell density in the heart. Values are the mean ± SEM. *$p < 0.05$ versus the sham group. **b** Immunostaining with an anti-histamine antibody. **a** Representative staining of a heart from the sham group. **b** Representative staining of a heart from the control group. **c** Negative control section incubated without the primary antibody. The *scale bars* indicate 50 μm

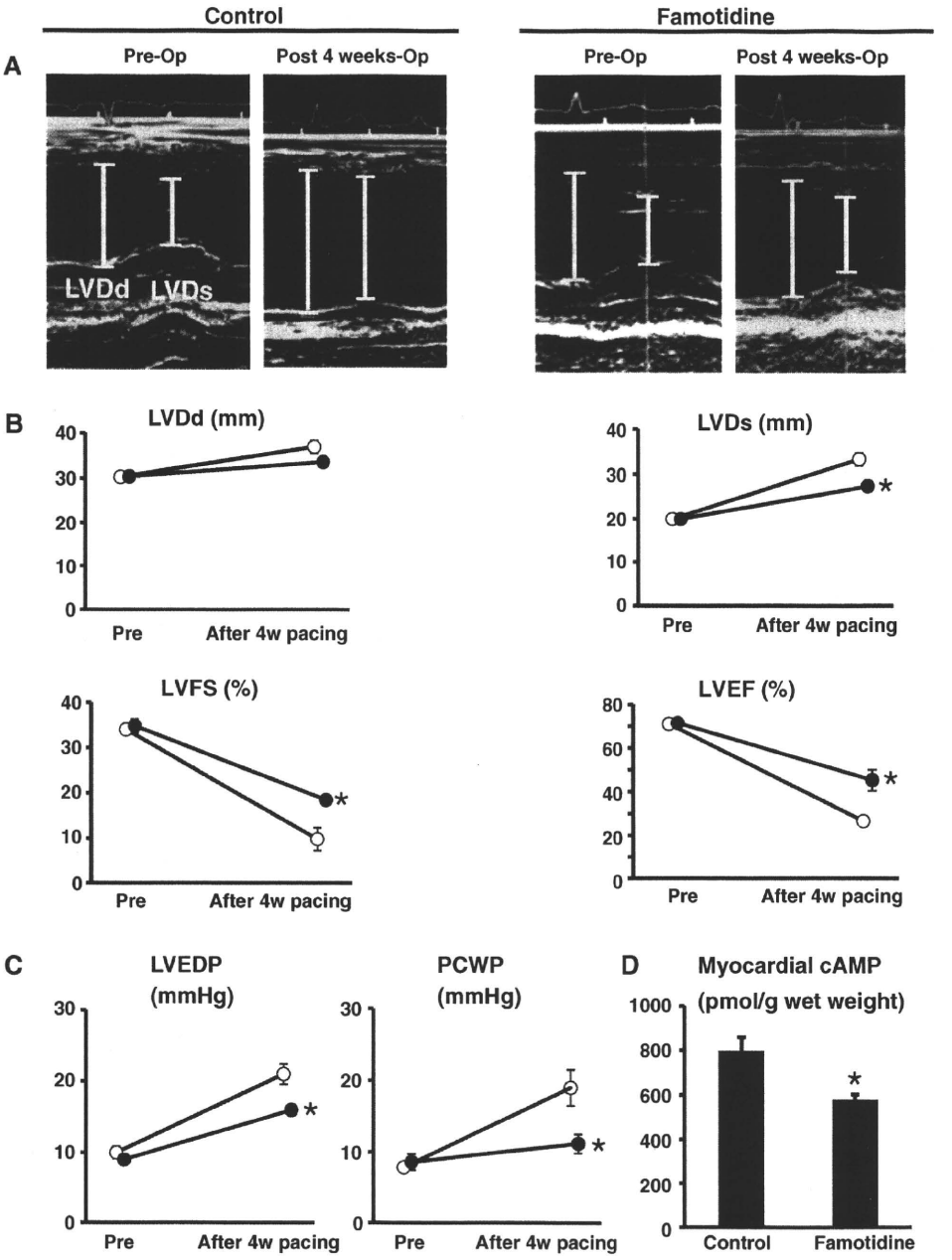


**Fig. 2** Effects of famotidine on echocardiographic and hemodynamic parameters and myocardial cAMP levels. **a** Representative 2D echocardiograms. **b** Quantitative analysis of echocardiographic parameters in the control and famotidine groups. *Open* and *closed circles* indicate the control group and the famotidine group, respectively. **c** LVEDP and mean PCWP in the control and famotidine groups. **d** Myocardial cAMP levels in each group. All values are the mean ± SEM. *$p < 0.05$ versus the sham group

117 ± 7 bpm, respectively), and the famotidine group (101 ± 3 mmHg and 115 ± 8 bpm, respectively). These parameters did not significantly differ among the groups. LV d*P*/d*t* was 3,592 ± 512 mmHg/s in the control group and 3,981 ± 528 mmHg/s in the famotidine group. Four weeks after surgery, neither hemodynamic nor echocardiographic data showed any changes compared with the preoperative values in the sham group (data not shown). Four weeks after rapid RV pacing, an administration of famotidine significantly limited the increase of both LVDd and LVDs, as well as the decrease of both LVFS and LVEF (33.4 ± 0.8 mm, 27.4 ± 1.2 mm, 18.5 ± 2.6% and 45.4 ± 4.8%, respectively), compared with the findings in the control group (37.0 ± 1.4 mm, 33.4 ± 1.4 mm, 9.9 ± 1.0% and 26.7 ± 2.4%, respectively) (Fig. 2a, b). Four weeks after RV pacing, LV end-diastolic pressure (LVEDP) and PCWP of the famotidine group (16 ± 2 and 11 ± 1 mmHg, respectively), were both significantly lower compared with the values in the control group (21 ± 2 and 19 ± 2 mmHg and, respectively) (Fig. 2c). LV d*P*/d*t* after RV pacing was significantly preserved higher in the famotidine group (2,601 ± 216 mmHg/s) compared with that in control group (2,077 ± 124 mmHg/s) ($p < 0.05$).

The myocardial cAMP level was significantly higher in the control group (796 ± 111 pmol/g wet weight) compared with that in the sham group (597 ± 77 pmol/g wet

weight), while it was significantly lower in the famotidine group (577 ± 28 pmol/g wet weight) compared with the control group ($p < 0.05$) (Fig. 2d).

### Additive effects of famotidine and a β-blocker on cardiac performance in dogs with pacing-induced heart failure

Before pacing, mean aortic pressure and heart rate were both similar in the carvedilol group (101 ± 7 mmHg and 111 ± 8 bpm, respectively), and the famotidine + carvedilol group (93 ± 2 mmHg, 106 ± 7 bpm, respectively), and these parameters did not significantly differ among the groups. LV d*P*/d*t* was 3,672 ± 417 mmHg/s in the carvedilol group and 3,941 ± 284 mmHg/s in the famotidine + carvedilol group. After rapid RV pacing for 4 weeks, both LVDd and LVDs were decreased and both LVFS and LVEF were increased (33 ± 0.4 mm, 25 ± 0.7 mm, 28 ± 2%, and 54 ± 3%, respectively), in the famotidine + carvedilol group compared with the respective values in the carvedilol group (34 ± 1 mm, 28 ± 1 mm, 23 ± 1%, and 38 ± 5%, respectively) (Fig. 3a).

Four weeks after RV pacing, LVEDP and PCWP of the carvedilol + famotidine group (12 ± 3 and 10 ± 4 mmHg, respectively), were both significantly reduced compared with the respective values in the carvedilol group (16 ± 2 and 15 ± 1 mmHg, respectively) (Fig. 3b). LV d*P*/d*t* after RV pacing was preserved higher in the famotidine + carvedilol group (3,382 ± 252 mmHg/s) compared with that in carvedilol group (2,740 ± 321 mmHg/s) ($p < 0.05$).

Furthermore, the myocardial cAMP level was significantly lower in the carvedilol + famotidine group (488 ± 45 pmol/g wet weight) compared with that in the carvedilol group (615 ± 28 pmol/g wet weight) (Fig. 3c).

## Discussion

In the present study, we demonstrated that (1) myocardial histamine expression was increased by pacing-induced heart failure, (2) the histamine $H_2$ receptor blocker famotidine improved cardiac performance (gauged by echocardiographic and hemodynamic parameters) along with a reduction of myocardial cAMP accumulation, and (3) there was an additive effect of combined histamine $H_2$ receptor and β-adrenergic receptor blockade on cardiac performance in dogs with pacing-induced heart failure.

### Impact of histamine blockade on cardiac failure

Histamine is one of the autacoids, and is stored and released by mast cells in the human heart, as well as in other organs or

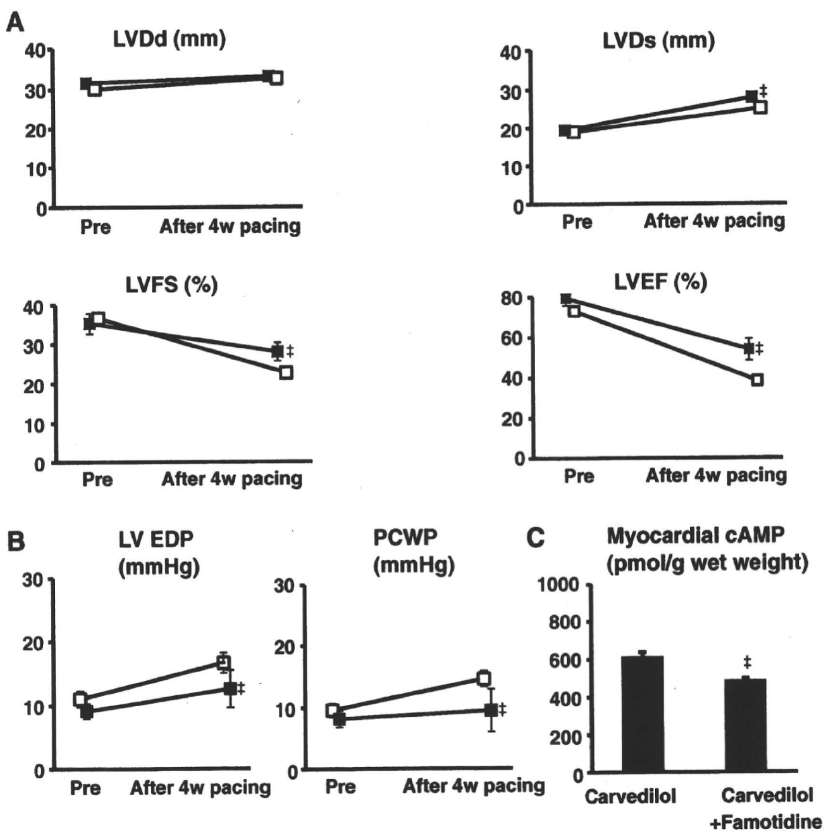


**Fig. 3** Additive effect of famotidine and carvedilol on cardiac performance. **a** Quantitative analysis of echocardiographic parameters in the carvedilol and carvedilol + famotidine groups. *Open* and *closed squares* indicate the carvedilol group and the carvedilol + famotidine group, respectively. **b** LVEDP and mean PCWP in the carvedilol group and carvedilol + famotidine group. *Open* and *closed squares* indicate the carvedilol group and the carvedilol + famotidine group, respectively. **c** Myocardial cAMP levels in each group. All values are the mean ± SEM. *$p < 0.05$ versus the carvedilol group

tissues [8]. Recently, the number of mast cells and the myocardial histamine level were found to increase in the hearts of patients with idiopathic dilated cardiomyopathy or ischemic cardiomyopathy [26]. Histamine modulates various cellular functions via the activation of four different G-protein-coupled receptors ($H_{1-4}$ receptors) [29]. As is well known, histamine $H_2$ receptors located on gastric cells promote the production of gastric acid [10] and histamine $H_2$ receptor blockers have been widely used for the treatment of peptic ulcer. Interestingly, histamine $H_2$ receptors are also expressed in canine and human ventricular myocardium [14, 18], although the expression levels were different among species [18]. Consisted with the previous studies, we confirmed the presence of histamine $H_2$ receptor in the canine heart using quantitative reverse-transcriptase PCR (data not shown).

In the present study, the precise locations of histamine receptors in myocytes or vessels in the canine hearts remained unclear. However, since famotidine did not decrease blood pressure in this study, the accumulating lines of evidence would suggest that histamine $H_2$ blockers did not have the potent effect on the vessels compared with cardiomyocytes. On the other hand, since histamine $H_1$ receptors are abundantly expressed in the vessels in most animal species [29], histamine $H_1$ receptor blocker has the effects on vessels. In addition, stimulation of $H_2$ receptors transduces the intracellular signals via Gs protein, as does the stimulation of $\beta$-adrenergic receptors. Moreover, histamine has a positive inotropic effect on human ventricular myocardium and has been suggested to have a role in cardiovascular diseases [3, 11]. Although it was reported that the maximum inotropic effects of histamine receptor stimulation were less than those mediated by beta-adrenergic receptors [5, 35], the roles of histamine receptor blockade have remained unclear compared with those of beta-adrenergic receptor.

Based on these backgrounds, we previously proposed that histamine $H_2$ receptor blockers could provide a novel therapeutic strategy for heart failure, and we have reported that histamine $H_2$ blocker treatment may have a cardioprotective effect in patients with chronic heart failure [16]. In the present study, we found that myocardial histamine expression was increased in dogs with pacing-induced heart failure compared with that in sham dogs on immunohistochemical analysis. Also, the histamine $H_2$ receptor blocker, famotide, prevented the development of heart failure induced by rapid RV pacing and lessened the myocardial accumulation of cAMP. These findings suggest that histamine $H_2$ receptor blockade exerts a cardioprotective effect along with the amelioration of myocardial cAMP accumulation. Recently it was reported that increased cardiac adenylyl cyclase expression is associated with mortality after myocardial infarction in rats [31]. It has been controversial for the role of myocardial cAMP in the heart failure [17]. Although increased cAMP acutely induced the improvement of ventricular function, several trials with either beta-adrenergic agonists or PDE inhibitors have revealed an increase in mortality [17, 20]. In the present study, in the dogs with the drugs that decreases myocardial cAMP levels, the development of heart failure was substantially attenuated, however further investigation will be needed to solve the roles of cAMP in the onset and progression of heart failure.

### Additive effects of histamine $H_2$ blocker and $\beta$-blocker therapy on cardiac performance

$\beta$-Blockers have long been established as useful agents for chronic heart failure [2, 7, 25, 32]. These drugs act by preventing intracellular Ca overload, because $\beta$-adrenergic stimulation promotes Ca overload via Gs protein [34]. Histamine $H_2$ receptor blockade also prevents Ca overload [28], so we hypothesized that the combination of a histamine $H_2$ receptor blocker and a $\beta$-blocker would exert a stronger cardioprotective effect than either agent alone. Almost all of the patients in our earlier study, which showed that histamine $H_2$ receptor blockers were effective for the treatment of CHF, were also on $\beta$-blocker therapy [16], suggesting that there was an additive effect of histamine $H_2$ receptor and $\beta$-adrenergic receptor blockade in patients with CHF. In the present study, we demonstrated that the combination of a histamine $H_2$ receptor blocker and a $\beta$-blocker prevented the development of heart failure compared with $\beta$-blocker monotherapy. Thus, histamine $H_2$ receptor blockers have a potential clinical role in the treatment of CHF.

### Rationale of the present study

The present study provided strong experimental evidence that histamine $H_2$ receptor blockade improves the pathophysiology of CHF. We have already reported about the beneficial effects of famotidine in patients with heart failure [16]. However, clinical research may be confounded by unexpected errors due to (1) the influence of other drugs being used by patients with CHF, (2) variation in the severity of CHF between patients, and (3) variation in the duration of CHF. Therefore, it was important to prove that histamine $H_2$ receptor blockade improves CHF in a controlled experimental setting (canine cardiomyopathy model) to support the clinical use of famotidine for CHF. Furthermore, to determine the merit of famotidine in heart failure patients, the present study would be a basis to design a prospective randomized double-blinded study.

## Limitations

There are several limitations in this study. First, carvedilol blocks alpha$_1$-, beta$_1$-, beta$_2$- receptors, decreased the cardiac effects of norepinephrine, and has additional antioxidant and antiproliferative effects [4, 19]. In the present study, we did not address that carvedilol has the pleiotropic effects and is not just a beta-blocker.

Second, we did not measure cardiac output as a cardiac contractive index in the present study. However, we have previously reported that our tachycardia-induced heart failure model in dogs using the same procedure of the present study, revealed the low output state that mimics heart failure in human [27]. Our untreated dogs in the heart failure group were strongly suggested in the low output state because of decreased the level of ejection fraction as much as our previous study. In the present study, we analyzed the values of d$P$/d$t$ as the index of contractility by measuring LV pressure using a pig tail catheter.

In summary, despite these limitations, we demonstrated that the histamine $H_2$ receptor blockade preserves cardiac systolic function in dogs with pacing-induced heart failure, even in the presence of $\beta$-adrenergic receptor blockade. This finding strengthens the rationale for the beneficial effects of histamine $H_2$ blockers in the treatment of heart failure.

**Acknowledgments** The authors thank Akiko Ogai for technical assistance; Masahiko Takahashi (Astellas Co. Ltd.) for providing information on famotidine; and the Evidence Finders' Club for their encouragement of this study. This work was supported by a Grant-in-aid from the Japanese Ministry of Health, Labor, and Welfare; a Grant-in-aid from the Japanese Ministry of Education, Culture, Sports, Science and Technology; a Grant from the Japan Heart Foundation; and a Grant from the Japan Cardiovascular Research Foundation.

**Conflict of interest** None.

## References

1. Asanuma H, Minamino T, Ogai A, Kim J, Asakura M, Komamura K, Sanada S, Fujita M, Hirata A, Wakeno M, Tsukamoto O, Shinozaki Y, Myoishi M, Takashima S, Tomoike H, Kitakaze M (2006) Blockade of histamine $H_2$ receptors protects the heart against ischemia and reperfusion injury in dogs. J Mol Cell Cardiol 40:666–674
2. Bristow MR, Gilbert EM, Abraham WT, Adams KF, Fowler MB, Hershberger RE, Kubo SH, Narahara KA, Ingersoll H, Krueger S, Krueger S, Young S, Shusterman N (1996) Carvedilol produces dose-related improvements in left ventricular function and survival in subjects with chronic heart failure. Circulation 94:2807–2816
3. Bristow MR, Ginsburg R, Harrison DC (1982) Histamine and the human heart: the other receptor system. Am J Cardiol 49:249–251
4. Bristow MR (1997) Mechanism of action of beta-blocking agents in heart failure. Am J Cardiol 80:26L–40L
5. Brodde OE, Hillemann S, Kunde K, Vogelsang M, Zerkoski HR (1992) Receptor systems affecting force of contraction in the human heart and their alterations in chronic heart failure. J Heart Lung Transplant 11:S164–S174
6. Brown L, Lorenz B, Erdmann E (1986) Reduced positive inotropic effects in diseased human ventricular myocardium. Cardiovasc Res 20:516–520
7. CIBIS II Investigators and Committees (1999) The cardiac insufficiency bisoprolol study II (CIBIS II): a randomized trial. Lancet 353:9–13
8. Dvorak AM (1986) Mast-cell degranulation in human hearts. N Engl J Med 315:969–970
9. Eichhorn EJ (1998) Restoring function in failing hearts: the effects of beta blockers. Am J Med 104:163–169
10. Gantz I, Schaffer M, DelValle J, Logsdon C, Campbell V, Uhier M, Yamada T (1991) Molecular cloning of a gene encoding the histamine $H_2$ receptor. Proc Natl Acad Sci USA 88:5937
11. Hara M, Ono K, Hwang MW, Iwasaki A, Okada M, Nakatani K, Sasayama S, Matsumori A (2002) Evidence for a role of mast cells in the evolution to congestive heart failure. J Exp Med 195:375–381
12. Hattori Y (1999) Cardiac histamine receptors: their pharmacological consequences and signal transduction pathways. Methods Find Exp Clin Pharmacol 21:123–131
13. Hinrichsen H, Halabi A, Kirsch W (1990) Hemodynamic effects of different $H_2$-receptor antagonists. Clin Pharmacol Ther 48:302–308
14. Hill SJ, Ganellin CR, Timmerman H, Schwartz JC, Shankley NP, Young JM, Schunack W, Levi R, Haas HL (1997) International Union of Pharmacology. XIII. Classification of histamine receptors. Pharmacol Rev 49:253–278
15. Jessup M, Brozena S (2003) Heart failure. N Engl J Med 348:2007–2018
16. Kim J, Ogai A, Nakatani S, Hashimura K, Kanzaki H, Komamura K, Asakura M, Asanuma H, Kitamura S, Tomoike H, Kitakaze M (2006) Impact of blockade of histamine $H_2$ receptors on chronic heart failure revealed by retrospective and prospective randomized studies. J Am Coll Cardiol 48:1378–1384
17. Leineweber K, Bohm M, Heusch G (2006) Cyclic adenosine monophosphate in acute myocardial infarction with heart failure Slayer or savior? Circulation 114:365–367
18. Matsuda N, Jesmin S, Takahashi Y, Hatta E, Kobayashi M, Matsuyama K, Kawakami N, Sakuma I, Gando S, Fukui H, Hattori Y, Levi R (2004) Histamine $H_1$ and $H_2$ receptor gene and protein levels are differentially expressed in the hearts of rodents and humans. J Pharmacol Exp Ther 309:786–795
19. Metra M, Giubbini R, Nodari S, Boldi E, Modena MG, Cas LD (2000) Differential effects of beta-blockers in patients with heart failure. Circulation 102:546–551
20. Movsesian MA (1999) Beta-adrenergic receptor agonists and cyclic nucleotide phosphodiesterase inhibitors: shifting the focus from inotropy to cyclic adenosine monophosphatase. J Am Coll Cardiol 34:318–324
21. Nault MA, Milne B, Parlow JP (2002) Effects of the selective $H_1$ and $H_2$ histamine receptor antagonists loratadine and ranitidine on autonomic control of the heart. Anesthesiology 96:336–341
22. Neumann T, Heusch G (1997) Myocardial, skeletal muscle, and renal blood flow during exercise in conscious dogs with heart failure. Am J Physiol 273:H2452–H2457
23. Neumann T, Vollmer A, Schaffner TH, Hess OM, Heusch G (1999) Diastolic dysfunction and collagen structure in canine pacing-induced heart failure. J Mol Cell Cardiol 31:179–192
24. Okada K, Minamino T, Tsukamoto Y, Liao Y, Tsukamoto O, Takashima S, Hirata A, Fujita M, Nagamachi Y, Nakatani T,

Yutani C, Ozawa K, Ogawa S, Tomoike H, Hori M, Kitakaze M (2004) Prolonged endoplasmic reticulum stress in hypertrophic and failing heart after aortic constriction: possible contribution of endoplasmic reticulum stress to cardiac myocyte apoptosis. Circulation 110:705–712

25. Packer M, Coats AJ, Fowler MB, Fowler MB, Katus HA, Krum H, Mohacsi P, Rouleau JL, Tendera M, Castaigne A, Roecker EB, Schultz MK, DeMets DL, Carvedilol Prospective Randomized Cumulative Survival Study group (2001) Effect of carvedilol on survival in severe chronic heart failure. N Engl J Med 344:1651–1658
26. Patella V, Marino I, Arbustini E, Lamparter-Schummert B, Verga L, Adt M, Marone G (1998) Stem cell factor in mast cells and increased mast cell density in idiopathic and ischemic cardiomyopathy. Circulation 97:971–978
27. Sasaki H, Asanuma H, Fujita M, Takahama H, Wakeno M, Ito S, Ogai A, Asakura M, Kim J, Minamino T, Takashima S, Sanada S, Sugimachi M, Komamura K, Mochizuki N, Kitakaze M (2009) Metformin prevents progression of heart failure in dogs: role of AMP-activated protein kinase. Circulation 119:2568–2577
28. Schultz G, Rosenthal W, Hescheler J (1990) Role of G proteins in calcium channel modulation. Annu Rev Physiol 52:275–292
29. Simons FE (2004) Advances in $H_1$-antihistamines. N Engl J Med 351:2203–2217
30. Sugiyama A, Satoh Y, Takahara A, Nakamura Y, Shimizu-Sasamata M, Sato S, Miyata K, Hashimoto K (2003) Famotidine does not induce long QT syndrome: experimental evidence from in vitro and in vivo test systems. Eur J Pharmacol 466:137–146
31. Takahashi T, Tang T, Lai C, Roth DM, Rebolledo B, Saito M, Lew WYW, Clopton P, Hammond K (2006) Increased cardiac adenylyl cyclase expression is associated with increased survival after myocardial infarction. Circulation 114:388–396
32. The MERIT-HF Study Group (1999) Effect of metoprolol CR/XL in chronic heart failure: Metoprolol CR/XL Randomized Intervention Trial in Congestive Heart Failure (MERIT-HF). Lancet 353:2001–2007
33. Trautwein W, Hescheler J (1990) Regulation of cardiac L-type calcium current by phosphorylation and G proteins. Annu Rev Physiol 52:257–274
34. Xiao RP, Cheng H, Zhou YY, Kuschel M, Lakatta EG (1999) Recent advances in cardiac beta(2)-adrenergic signal transduction. Circ Res 85:1092–1100
35. Zeekowski HR, Broede A, Kunde K, Hillemann S, Schafer E, Vogelsang M, Michel MC, Brodde OE (1993) Comparison of the positive inotropic effects of serotonin, histamine, angiotensin II, endothelin and isoprenaline in the isolated human right atrium. Naunyn-Schemiedeberg's Arch Phamacol 347:347–352
36. Zhou R, Moench P, Heran C, Lu X, Mathias N, Faria TN, Wall DA, Hussain MA, Smith RL, Sun D (2005) pH-dependent dissolution in vitro and absorption in vivo of weakly basic drugs: development of canine model. Pharm Res 22:188–192

Journal of the American College of Cardiology
© 2009 by the American College of Cardiology Foundation
Published by Elsevier Inc.

Vol. 53, No. 22, 2009
ISSN 0735-1097/09/$36.00
doi:10.1016/j.jacc.2009.02.038



# Natriuretic Peptides Enhance the Production of Adiponectin in Human Adipocytes and in Patients With Chronic Heart Failure

Osamu Tsukamoto, MD, PHD,*‡ Masashi Fujita, MD, PHD,‡ Mahoto Kato, MD,* Satoru Yamazaki, PHD,* Yoshihiro Asano, MD, PHD,‡ Akiko Ogai, PHD,* Hidetoshi Okazaki, MD, PHD,* Mitsutoshi Asai, MD,‡ Yoko Nagamachi, BS,‡ Norikazu Maeda, MD, PHD,§ Yasunori Shintani, MD, PHD,‡ Tetsuo Minamino, MD, PHD,‡ Masanori Asakura, MD, PHD,* Ichiro Kishimoto, MD, PHD,† Tohru Funahashi, MD, PHD,§ Hitonobu Tomoike, MD, PHD,* Masafumi Kitakaze, MD, PHD*

*Suita, Osaka, Japan*

**Objectives** We investigated the functional relationship between natriuretic peptides and adiponectin by performing both experimental and clinical studies.

**Background** Natriuretic peptides are promising candidates for the treatment of congestive heart failure (CHF) because of their wide range of beneficial effects on the cardiovascular system. Adiponectin is a cytokine derived from adipose tissue with various cardiovascular-protective effects that has been reported to show a positive association with plasma brain natriuretic peptide (BNP) levels in patients with heart failure.

**Methods** The expression of adiponectin messenger ribonucleic acid (mRNA) and its secretion were examined after atrial natriuretic peptide (ANP) or BNP was added to primary cultures of human adipocytes in the presence or absence of HS142-1 (a functional type A guanylyl cyclase receptor antagonist). Changes of the plasma adiponectin level were determined in 30 patients with CHF who were randomized to receive intravenous ANP (0.025 μg/kg/min human ANP for 3 days, n = 15) or saline (n = 15).

**Results** Both ANP and BNP dose-dependently enhanced the expression of adiponectin mRNA and its secretion, whereas such enhancement was inhibited by pre-treatment with HS142-1. The plasma adiponectin level was increased at 4 days after administration of human ANP compared with the baseline value (from 6.56 ± 0.40 μg/ml to 7.34 ± 0.47 μg/ml, $p < 0.05$), whereas there was no change of adiponectin in the saline group (from 6.53 ± 0.57 μg/ml to 6.55 ± 0.56 μg/ml).

**Conclusions** Natriuretic peptides enhance adiponectin production by human adipocytes in vitro and even in patients with CHF, which might have a beneficial effect on cardiomyocytes in patients receiving recombinant natriuretic peptide therapy for heart failure. (J Am Coll Cardiol 2009;53:2070–7) © 2009 by the American College of Cardiology Foundation

Plasma natriuretic peptide levels are increased in patients with congestive heart failure (CHF), and the measurement of these peptides is used widely to assess the presence, severity, and prognosis of CHF (1,2). Both atrial natriuretic peptide and brain natriuretic peptide (ANP and BNP, respectively) have a beneficial effect in patients with heart failure because of their various biological actions (3–5).

See page 2078

Adiponectin is a circulating cytokine derived from adipose tissue that has attracted considerable interest because of its identification as a risk factor for cardiovascular disease (6,7) and CHF (8). Adiponectin production is down-regulated in patients with coronary risk factors that are associated with the development of heart failure (9,10).

From the Cardiovascular Division of *Medicine and †Biochemistry, National Cardiovascular Center, Suita, Osaka, Japan; and the Departments of ‡Cardiovascular Medicine and §Metabolic Medicine, Osaka University Graduate School of Medicine, Suita, Osaka, Japan. This work is supported by grants-in-aid from the Ministry of Health, Labor, and Welfare-Japan, grants-in-aid from the Ministry of Education, Culture, Sports, Science and Technology-Japan, grants from the Japan Heart Foundation, and grants from the Japan Cardiovascular Research Foundation (all to Dr. Kitakaze) and Takeda Medical Research Foundation (to Dr. Funahashi). Drs. Tsukamoto, Fujita, and Kato contributed equally to this work.

Manuscript received August 27, 2008; revised manuscript received January 22, 2009, accepted February 19, 2009.

Recently, adiponectin was reported to have a cardioprotective effect against ischemia-reperfusion injury (11) and hemodynamic stress (12,13) in mice. Interestingly, it has been reported that the level of N-terminal pro-brain natriuretic peptide shows a positive correlation with the plasma adiponectin concentration in patients with chronic heart failure (14).

Given these experimental and clinical observations, we hypothesized that natriuretic peptides might increase adiponectin production in patients with heart failure to protect the cardiovascular system. Accordingly, in the present study, we investigated whether natriuretic peptides could directly increase adiponectin production by these adipocytes (and the cellular mechanisms involved) and confirmed this effect on adiponectin in the clinical setting.

## Methods

**Agents.** Both human ANP and BNP were purchased from Sigma-Aldrich (St. Louis, Missouri). HS142-1, a functional guanylyl cyclase-A type receptor antagonist, was provided by Kyowa Hakko Kogyo Co., Ltd. (Mishima, Japan). A cGMP analog (8-pCPT-cGMP) and a selective cGMP-dependent protein kinase G (PKG) inhibitor ($R_p$-8-Br-PET-cGMP-S) were obtained from Biolog Life Science Institute (Bremen, Germany). An antibody directed against mouse adiponectin (MAB3608) was purchased from Chemicon International, Inc.

**Primary culture and in vitro study of human adipocytes.** Subcutaneous adipocytes derived from the adipose tissue of 6 women were obtained commercially together with culture medium from Zen-Bio, Inc. (Research Triangle Park, North Carolina. The donors were nonsmokers with a mean body mass index of 27.0 kg/m$^2$ (range 25.9 to 29.1 kg/m$^2$) and an average age of 47 years (range 29 to 63 years). Cells were maintained in adipocytes maintenance medium (i.e., AM-1) containing Dulbecco's modified Eagle medium/Ham's F-12 (1:1, v/v), 3% fetal calf serum, 15 mmol/l HEPES (pH 7.4), biotin, pantothenate, human insulin, 1 μmol/l dexamethasone, 100 U/ml penicillin, 100 μg/ml streptomycin, and 0.25 μg/ml amphotericin B at 37°C in a humidified atmosphere of 95% air/5% $CO_2$. The medium was changed every 2 days. Primary cultures of the adipocytes were used to examine the effects of natriuretic peptides (ANP or BNP) on the expression of adiponectin.

Before these experiments, the cells were plated in adipocyte basal medium (i.e., BM-1) containing Dulbecco's modified Eagle medium/Ham's F-12 (1:1, volume/volume), 15 mmol/l 4-(2-hydroxyethyl)-1-piperazineethanesulfonic acid (pH 7.4), biotin, and pantothenate for 24 h. Then the indicated concentrations of either natriuretic peptide (from $10^{-11}$ to $10^{-9}$ mol/l) were added to the BM-1 medium. After 24 h of incubation, the medium was harvested for Western blotting to measure the secretion of adiponectin, and the cells were also harvested for ribonucleic acid (RNA) analysis. The effect of each natriuretic peptide on adiponectin messenger ribonucleic acid (mRNA) levels was determined by quantitative real-time polymerase chain reaction (PCR).

**Measurement of adiponectin.** In patients with CHF, the plasma adiponectin concentration was measured by the use of an ELISA kit (Otsuka Pharmaceutical Co., Ltd., Tokyo, Japan) according to the manufacturer's protocol. Adiponectin secretion by primary cultured human adipocytes was assessed by Western blotting of the culture medium, as previously described (15), and the immunoreactive bands were quantified by densitometry (Molecular Dynamics, Sunnyvale, California).

**Abbreviations and Acronyms**

ANP = atrial natriuretic peptide
BNP = brain natriuretic peptide
CHF = congestive heart failure
GC-A = type A guanylyl cyclase receptor
hANP = human atrial natriuretic peptide
NPR = natriuretic peptide receptor
PKG = protein kinase G

**Reverse transcriptional-PCR.** Total RNA was extracted from adipocytes derived from human white fat with the use of RNA-Bee-RNA Isolation Reagent (Tel-Test, Inc., Gainesville, Florida). Then, 200 ng of total RNA was reversed transcribed and amplified by the use of an Omniscript RT kit (Qiagen, Hilden, Germany) according to the manufacturer's protocol. The forward primers for type A guanylyl cyclase receptor (GC-A) and natriuretic peptide receptor (NPR)-C were 5′-CCAGTTCCAAGTCTTTGCCAAGACAGCA and 5′-GGAAGACATCGTGCGCAATA, respectively, and the reverse primers for GC-A and NPR-C were 5′-CATTGTGTAGAAACAGCATGCCCTTGACGA and 5′-TGCTCCGGATGGTGTCACT, respectively. As a positive control, we used the samples of human cardiac tissue under the protocol approved by the institutional review board of the National Cardiovascular Center (No. 14-18) (16).

**Quantitative real-time PCR analysis.** Quantitative real-time PCR was performed as described previously (17). Oligonucleotide primers and TaqMan probes for human adiponectin and glyceraldehyde 3-phosphate dehydrogenase were purchased from Applied Biosystems (Foster City, California).

**Subjects and design of the clinical study.** We prospectively studied 30 consecutive CHF patients who were admitted to the emergency department of the National Cardiovascular Center between April and July 2006. The exclusion criteria were as follows: age >80 years, cardiogenic shock or hypotension (systolic blood pressure <100 mm Hg), and renal failure (serum creatinine >2.0 mg/dl). This study was approved by the Committee on Human Investigation of the National Cardiovascular Center, and all patients who participated gave informed consent. The 30 patients were randomized to 2 groups, a human atrial natriuretic peptide (hANP) group consisting of 15 patients who received administration of hANP and a control group consisting of 15 patients who were administered saline. In the hANP group, from immediately after the diagnosis of

JACC Vol. 53, No. 22, 2009
June 2, 2009:2070–7

acute exacerbation of CHF, hANP (0.025 μg/kg/min) was infused intravenously for 3 days. The study protocol did not restrict or specify any other diagnostic or therapeutic strategies. Blood for measuring the plasma adiponectin level was sampled before and 1 and 7 days after finishing the administration of hANP or saline (days 1, 4, and 10, respectively) (Fig. 3A).

**Statistical analysis.** For analysis of differences between the various treatments of adipocytes, analysis of variance was performed, followed by the appropriate post-hoc test. The differences in adiponectin levels between days 1 and 4 in each group were tested with a paired *t* test. The changes in adiponectin levels from day 1 to 4 between ANP group and saline group was tested with an unpaired *t* test. Results are expressed as the mean ± SEM, and p values of $<0.05$ were considered significant.

## Results

**Effect of natriuretic peptides on the expression and secretion of adiponectin by primary cultured human adipocytes.** First, we checked the expression of GC-A and NPR-C mRNA by using reverse transcriptional-PCR. As shown in Figure 1A, both GC-A and NPR-C mRNA was detectable in primary cultured human adipocytes. To investigate the effects of natriuretic peptides on the regulation of adiponectin production in adipocytes, we incubated primary cultured human adipocytes with recombinant ANP. When ANP was used at a concentration of $10^{-10}$ mol/l (pathological plasma concentration), it increased adiponectin mRNA expression after 6 h of incubation and reached a maximum after 12 h (Fig. 1B). Next, we incubated human adipocytes with ANP at the concentration of from $10^{-11}$ mol/l (normal plasma concentration) to $10^{-9}$ mol/l (pharmacological plasma concentrations) and demonstrated enhanced adiponectin mRNA expression and adiponectin secretion into the medium in a dose-dependent manner, whereas these changes were completely inhibited by pretreatment with HS142-1 (Figs. 1C and 1D). Incubation of adipocytes with BNP also increased the expression of adiponectin mRNA in a dose-dependent manner and this effect was completely blocked by pretreatment with HS142-1 (Figs. 1E and 1F).

**Involvement of cGMP/PKG signaling in natriuretic peptide-induced synthesis of adiponectin.** Because both ANP and BNP exert their biological effects by promoting cGMP production, to investigate the role of the GC-A/cGMP/PKG signaling pathway in adiponectin production, we measured the changes of cGMP in ANP-treated primary cultured human adipocytes. We found that incubation with ANP increased the cGMP level and that this effect was blunted by co-treatment with HS142-1 (data not shown). Next, we treated human adipocytes with the cGMP analog 8-pCPT-cGMP and the PKG inhibitor ($R_p$)-8-Br-PET-cGMP-S. The activation of PKG by 8-pCPT-cGMP (50 μmol/l for 12 h) produced an increase of adiponectin mRNA expression similar to that observed after incubation with ANP. The effect of ANP on adiponectin mRNA expression was abolished in the presence of ($R_p$)-8-Br-PET-cGMP-S (100 nmol/l) (Fig. 2A). Consistent with these findings, adiponectin secretion into the culture medium also was increased by stimulation of the cGMP/PKG-dependent pathway (Fig. 2B). These results suggested that natriuretic peptides promote adiponectin synthesis via the GC-A/cGMP/PKG-dependent pathway.

**Increase of plasma adiponectin levels in CHF patients treated with hANP.** To confirm the effect of natriuretic peptides on the production of adiponectin, we conducted the clinical study. Thirty consecutive patients who met the inclusion criteria were enrolled in this clinical study. Fifteen patients were randomized to the ANP group, and 15 were assigned to the saline group. Baseline variables and treatments of the 2 groups are shown in Table 1. There were no differences in baseline clinical characteristics, hemodynamics, biochemical data, or medications. There was also no significant difference in the baseline plasma level of adiponectin between the 2 groups. As shown in Figure 3B, the plasma level of adiponectin did not change throughout the study in the saline group. On the other hand, the plasma adiponectin level at 1 day after finishing the administration of hANP (day 4) was significantly increased compared with the baseline value (day 1) in the ANP group, and it returned to baseline by 7 days after the completion of hANP infusion (day 10). These results suggested that hANP infusion led to an increase of the plasma adiponectin level in patients with CHF.

## Discussion

In the present study, we demonstrated a novel effect of natriuretic peptides (ANP and BNP) on the production of adiponectin by adipocytes in both experimental and clinical studies. First, we clearly demonstrated that pathophysiological and pharmacological concentrations of either ANP or BNP increased adiponectin synthesis by primary cultured human adipocytes. Second, we showed that administration of recombinant ANP increased the plasma adiponectin level in patients with CHF.

ANP and BNP play an important role in the regulation of cardiovascular homeostasis. Their actions are primarily mediated via GC-A, which is expressed in various tissues and organs, including the kidneys, blood vessels, adrenal glands, and heart (18). Consistent with a previous report (19), we demonstrated that GC-A and NPR-C are expressed by human adipocytes. In the present study, we demonstrated a novel effect of both ANP and BNP on primary cultured human adipocytes, which was that pathophysiological or pharmacological concentrations of both peptides augmented adiponectin production by human adipocytes, with this effect being inhibited by treatment with HS142-1. Furthermore, we demonstrated that natriuretic peptides augment the production of adiponectin via a cGMP-dependent

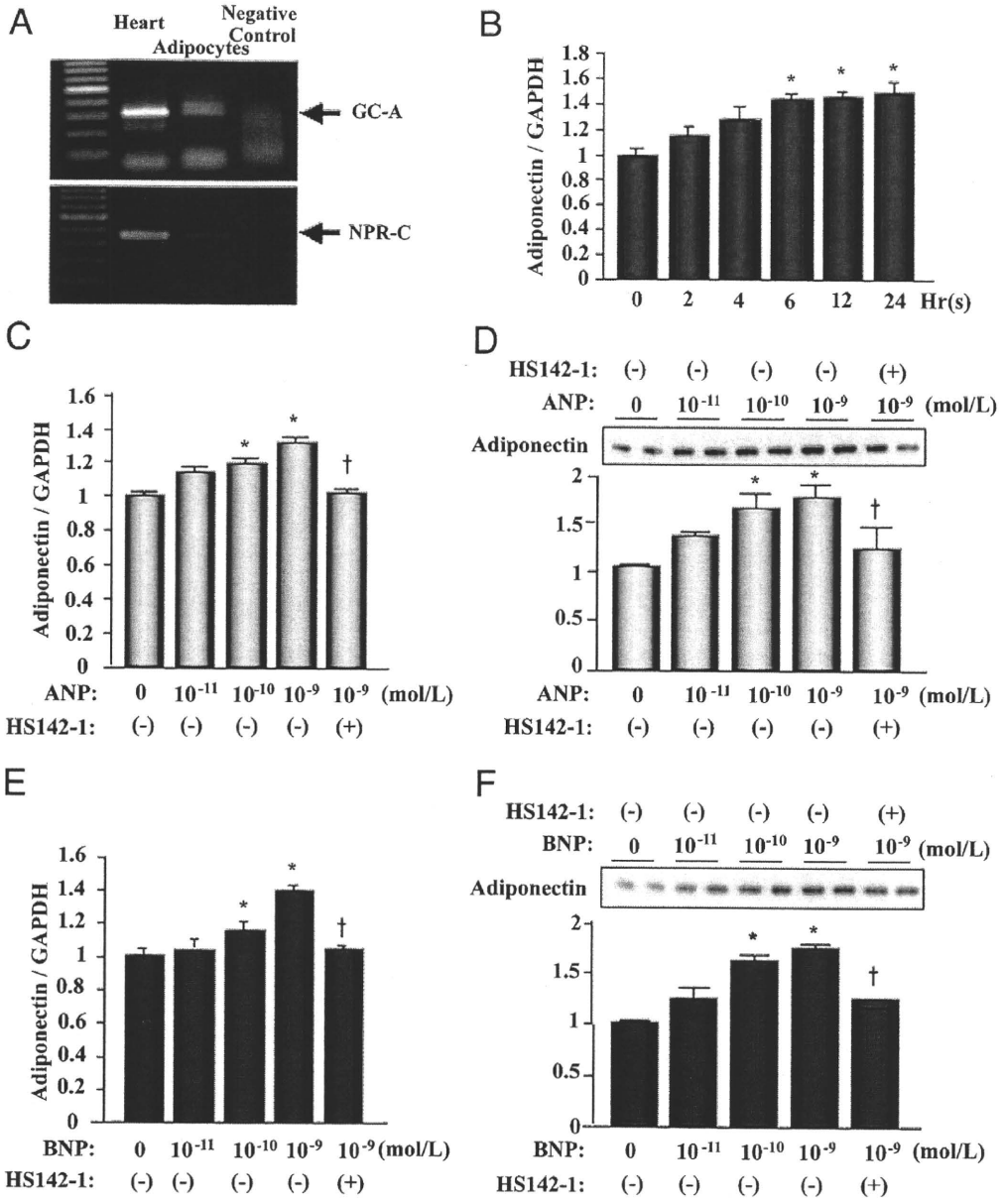


**Figure 1** Effect of Natriuretic Peptides on the Expression and Secretion of Adiponectin by Primary Human Adipocytes

**(A)** Expression of GC-A receptors **(top)** and NPR-C **(bottom)** mRNA by primary cultured human adipocytes. Reverse-transcription PCR revealed expression of both GC-A receptors and NPR-C by human adipocytes. **(B)** Effect of ANP ($10^{-10}$ mol/l) on the expression of adiponectin mRNA as determined by quantitative real-time PCR. **(C)** Dose-dependent effect of ANP on adiponectin mRNA expression, as determined by quantitative real-time PCR. Human adipocytes were treated with the indicated concentrations of ANP for 24 h. **(D)** Dose-dependent effect of ANP on adiponectin secretion into the culture medium. **(Top)** A representative Western blot of adiponectin. **(Bottom)** Quantitative analysis of adiponectin by densitometry. Values are normalized to the control. *$p < 0.05$ versus control, †$p < 0.05$ versus ANP $10^{-9}$ mol/l. **(E)** Dose-dependent effect of BNP on adiponectin mRNA expression, as determined by quantitative real-time PCR. **(F)** Dose-dependent effect of BNP on adiponectin secretion into the culture medium as determined by Western blotting. **(Top)** Representative Western blot of adiponectin. **(Bottom)** Quantitative analysis of adiponectin by densitometry. Values are normalized to the control. *$p < 0.05$ versus control. †$p < 0.05$ versus BNP $10^{-9}$ mol/l. ANP = atrial natriuretic peptide; BNP = brain natriuretic peptide; GC-A = type A guanylyl cyclase receptor; mRNA = messenger ribonucleic acid; NPR-C = natriuretic peptide receptor C; PCR = polymerase chain reaction.

pathway. These findings are important evidence that ANP and BNP regulate adiponectin production by human adipocytes.

Intravenous infusion of nesiritide (recombinant human BNP) has been reported to have beneficial hemodynamic effects in patients with CHF (4,5). The use of ANP also has been reported to have beneficial effects in patients with acute myocardial infarction (20,21). These beneficial effects have been attributed to the cardiovascular-protective actions of natriuretic peptides, including diuresis, natriuresis, vaso-

JACC Vol. 53, No. 22, 2009
June 2, 2009:2070–7

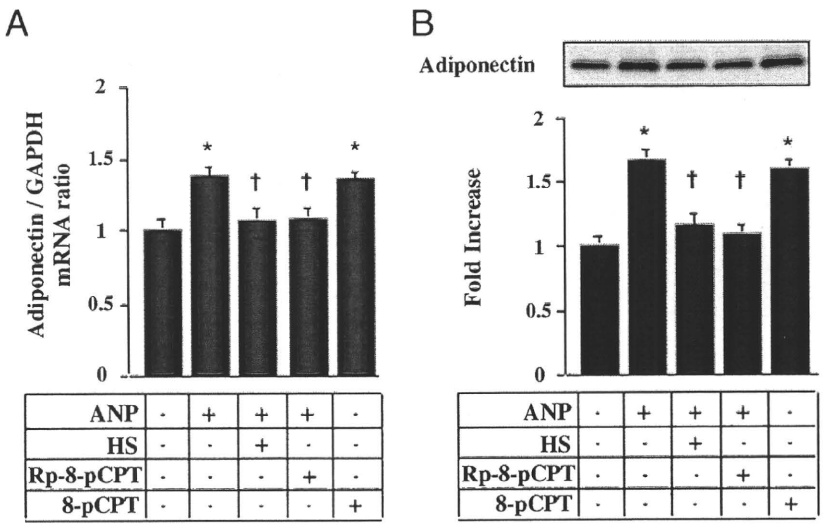


**Figure 2** Involvement of the cGMP/PKG Signaling Pathway in the Induction of Adiponectin Synthesis by ANP

**(A, B)** Involvement of PKG was assessed by the treatment of primary cultured human adipocytes with 8-pCPT-cGMP (8-pCPT) and ($R_p$)-8-Br-PET-cGMP-S (Rp-8-pCPT). Adiponectin mRNA levels were determined by quantitative real-time PCR **(A)** and secretion of adiponectin into the culture medium was determined by Western blotting. Quantitative analysis of adiponectin secretion into the culture medium was done by densitometry **(B)**. Values are normalized to the control. *p < 0.05 versus control. †p < 0.05 versus ANP. HS = HS142-1; other abbreviations as in Figure 1.

dilation, and reduction of activity of the sympathetic nervous system and the renin-angiotensin-aldosterone system (3–5). In the present study, we administered recombinant ANP to patients with CHF and observed the changes of plasma adiponectin. The plasma adiponectin level of the ANP group was increased at 1 day after the finish of ANP administration compared with that in the control group, and then returned to baseline by 7 days after the completion of administration in patients with CHF.

Importantly, Moro et al. (22) showed that ANP did not affect the secretion of adiponectin in human abdominal adipose tissue from overweight women. This result may appear contradict ours, but we believe that is not the case. First, the concentration of ANP they used ($10^{-6}$ mol/l) in the experiment of cultured adipocytes was greater than our concentration. Second, our data that recombinant ANP increased the plasma adiponectin levels were drawn from patients with heart failure, whereas the data of Moro et al. (22) were from cultured fat tissues of overweight women who underwent plastic surgery. However, they also demonstrated the potential stimulatory effect of ANP on adiponectin production from human adipose tissue in the presence of

**Table 1** Clinical Characteristics of the 2 Groups

| | hANP Group (n = 15) | Saline Group (n = 15) | p Value |
|---|---|---|---|
| Age (yrs) | 60 ± 19 | 59 ± 19 | NS |
| Sex (male/female) | 9/6 | 10/5 | NS |
| Heart rate (beats/min) | 62 ± 11 | 66 ± 7 | NS |
| Body mass index (kg/m$^2$) | 21.4 ± 1.1 | 21.1 ± 1.7 | NS |
| Systolic blood pressure (mm Hg) | 116 ± 9 | 113 ± 9 | NS |
| Diastolic blood pressure (mm Hg) | 76 ± 12 | 74 ± 6 | NS |
| NYHA functional class (II/III) | 14/1 | 10/5 | NS |
| LVEF by echocardiography (%) | 32 ± 2 | 31 ± 8 | NS |
| Plasma BNP (pg/ml) | 506 ± 39 | 537 ± 33 | NS |
| Other medications n (%) | | | |
| Loop diuretics | 9 (60) | 10 (67) | NS |
| Spironolactone | 5 (33) | 8 (53) | NS |
| ACEI or ARB | 12 (80) | 11 (80) | NS |
| Beta-blockers | 13 (86) | 12 (80) | NS |

ACEI = angiotensin-converting enzyme inhibitors; ARB = angiotensin II receptor blockers; BNP = brain natriuretic peptide; hANP = human atrial natriuretic peptide; LVEF = left ventricular ejection fraction; NS = not significant; NYHA = New York Heart Association.

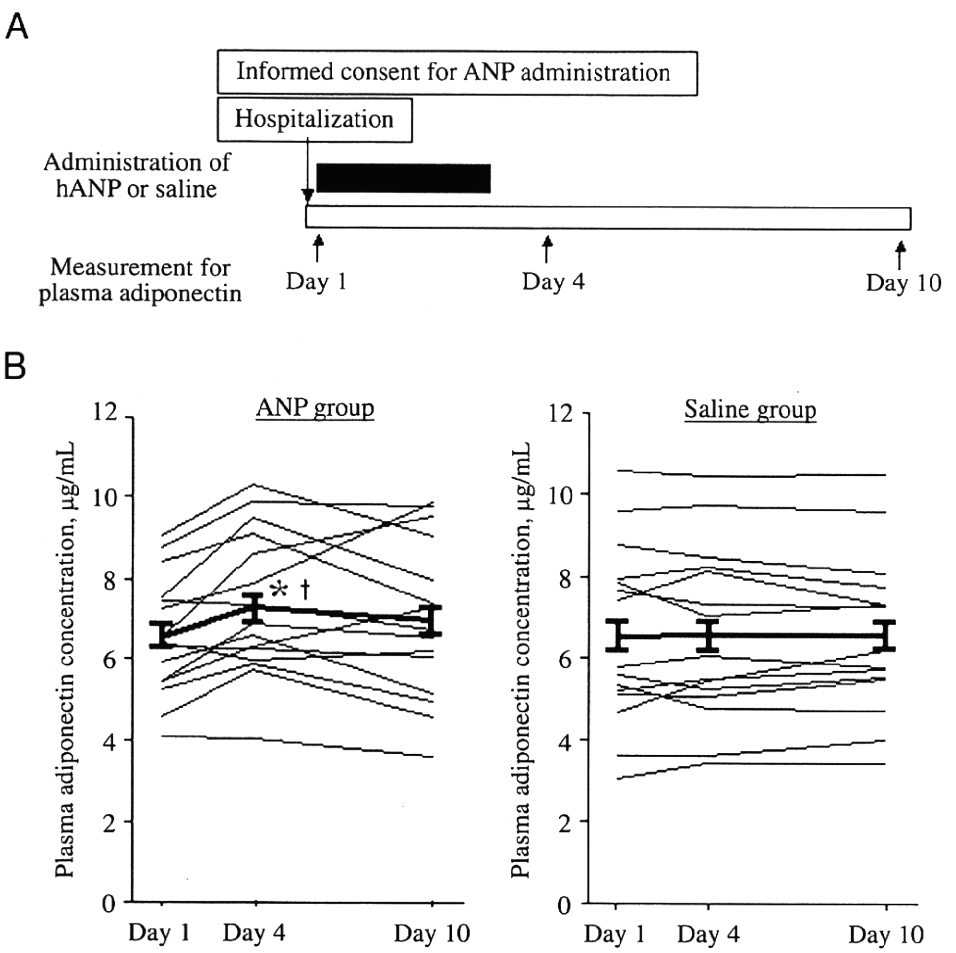


**Figure 3** Increased Plasma Adiponectin Level in Patients With CHF After ANP Treatment

**(A)** Outline of the study protocol. hANP or saline was infused continuously for 3 days in the ANP and saline groups, respectively. The **black bar** indicates administration of either hANP (0.025 μg/kg/min) or saline. **(B)** The plasma adiponectin concentration profile after treatment in both groups. *$p < 0.05$ versus baseline in the ANP group; †$p < 0.05$ versus at the corresponding time in the saline group. CHF = congestive heart failure; hANP = human atrial natriuretic peptide; other abbreviations as in Figure 1.

hormone-sensitive lipase inhibitor, which inhibits the formation of lipolysis-derived byproducts by ANP-induced lipolysis (22).

Recently, Yu et al. (23) demonstrated the increased ANP-induced lipolysis rates in large adipocytes compared with small adipocytes. Thus, the difference of adipocyte size between patients with CHF and obesity might contribute to the different pattern of adiponectin secretion. Finally, catecholamines also are involved in the control of lipolysis in humans (24). Thus, the prolonged exposure of high plasma level of catecholamines or the treatment with beta-adrenergic receptor blockers in patients with CHF also might affect the distinct pattern of adiponectin secretion from adipocytes. Although precise mechanisms are unknown, the human adipocytes could secrete adiponectin when the certain stress was loaded. However, it remains possible that factors such as tumor necrosis factor-alpha (25) and alpha-adrenergic stimulation (26), both of which are increased in patients with CHF, may influence the expression of adiponectin or that adiponectin levels are affected by medical treatment, so further investigations are needed.

It is not clear whether ANP augments the plasma adiponectin levels in healthy subjects because of the ethical problems. However, we have reported that the plasma adiponectin level increased along with an increase of plasma BNP levels in 1,538 healthy subjects (27). These results suggest that an increase of natriuretic peptides augments the plasma adiponectin levels and exerts a cardioprotective effect in clinical settings.

Under normal conditions the adult heart utilizes predominantly fatty acids to derive the majority of its energy (28). However, metabolic remodeling such as a marked shift in substrate preference away from fatty acids toward glucose is observed in hypertrophic and failing hearts and the decrease